ELECTRICAL AND OPTOELECTRONIC PROPERTIES OF HYDROGENATED SILICON FILMS PREPARED BY MICROWAVE GLOW-DISCHARGE

BY

© JOHN JAMES SCHELLENBERG

A THESIS

PRESENTED TO THE UNIVERSITY OF MANITOBA

IN PARTIAL FULFILLMENT OF THE

REQUIREMENTS FOR THE DEGREE OF

MASTER OF SCIENCE

IN

ELECTRICAL ENGINEERING

ISBN 0-315-34059-2

ELECTRICAL AND OPTOELECTRONIC PROPERTIES OF HYDROGENATED SILICON FILMS PREPARED BY MICROWAVE GLOW - DISCHARGE

BY

JOHN JAMES SCHELLENBERG

A thesis submitted to the Faculty of Graduate Studies of the University of Manitoba in partial fulfillment of the requirements of the degree of

MASTER OF SCIENCE

I hereby declare that I am the sole author of this thesis. I authorize the University of Manitoba to lend this thesis to other institutions or individuals for the purpose of scholarly research.

John James Schellenberg

I further authorize the University of Manitoba to reproduce this thesis by photocopying or by other means, in total or in part, at the request of other institutions or individuals for the purpose of scholarly research.

John James Schellenberg

ABSTRACT

We have reviewed the current theory on the dark conductivity and photoconductivity of a-Si:H thin films, including the processes of hopping, absorption, thermalization, quantum efficiency and electron recombination. We have also reviewed the recent literature dealing with the affect of temperature, light intensity, photon energy and electric field on the photoconductivity.

In the analysis of our observations, as reported in chapters three and four, we have found the following results. The films which are fabricated in conditions below electron cyclotron resonance (ECR) tend to be microcrystalline, whereas the films deposited in conditions above ECR will be amorphous. The films grown at ECR consist of two sizes of microcrystallites in an amorphous matrix. The dark conductivity and photoconductivity values are equal to the best quality RF films. For the amorphous (a-Si:H) films, the effects of temperature, light intensity and photon energy on the photoconductivity reveal the following characteristics of the localized gap states. As the equilibrium Fermi level decreases in the gap due to changing deposition conditions, the slope of the Urbach edge decreases and the structure at 1.3eV becomes sharper, eventually becoming a peak at E_{Fo}=0.96eV below E_c. These changes can be correlated to hydrogen incorporation. Above midgap, there is a maximum in the gap state density at 0.46eV below E_c and a minimum at 0.28ev below E_c.

New interpretations of both the light intensity dependence and the temperature dependence of the photoconductivity have been developed. We have reproduced an earlier equation due to Rose (1963), for several conditions, and therefore have shown that the equation has a broader use than previously supposed. As well, we have shown that the low temperature PC maximum is not necessarily caused by a change in the recombination levels.

ACKNOWLEDGEMENTS

Special thanks to everyone at the MDRL who have made the last few years so enjoyable, especially Bob Mcleod and Sergio Mejia. Special, special thanks to James White and Paul Shufflebotham for critical discussions throughout the last two years. Finally, I acknowledge the helpful interaction with, and guidance of, Dr. K.C. Kao.

TABLE OF CONTENTS

LIST OF FIGURES

CHAPTER 1: INTRODUCTION

A material which has a disordered structure can be described as vitreous, glassy, or amorphous. The word "amorphous" will be used to specify a disordered material which does not exhibit a definable thermodynamic phase (LeComber and Mort, 1971). Silicon does exist in four phases, however; these being the crystalline, polycrystalline, microcrystalline and amorphous phases. Structurally, the crystalline phase is defined as exhibiting long-range periodic atomic order, whereas the amorphous structure is defined as lacking this long-range order. In between these two extremes lie the other two phases. Polycrystalline silicon is composed of many large crystallites which are in random orientations, yet are in contact with each other. Microcrystalline silicon is composed of many smaller crystallites, each one either surrounded by amorphous silicon or in contact with other crystallites. An approximate crystallite size threshold is $\sim$300Å, below which the phase would be microcrystalline. Crystalline silicon (c-Si) is the best understood of the four phases and is the material commonly used for integrated circuits and other electronic devices.

The scientific study of a-Si began around 1965 and gained interest through the 1970's. One important problem which existed was the inability to dope the amorphous films. Because of the large concentration of gap states, caused by unfulfilled, or dangling, bonds, the Fermi level was pinned at a specific energy in the gap. In 1975, Spear et al (1975) were the first to incorporate n or p type dopants into a-Si:H by glow discharge in a gas mixture, such as PH_3 (phosphine) or B_2H_6 (Diborane). The

incorporation of hydrogen into silicon to form hydrogenated amorphous silicon (a-Si:H) was originally fabricated by Chittick et al (1969). Since that time a large research effort has been directed toward the study of the properties of both undoped and doped a-Si:H. This research effort has led to several device applications, including solar cells and xerographic films (Hamakawa, 1985; Oda et al, 1981), and to a new direction of research, such as quantum well and multilayer structures (Ogina et al, 1985).

Microcrystalline Silicon (μc-Si) was also discovered before 1970 (Veprek and Maracek, 1968) but did not gain immediate interest. Today, possible applications include its use in multilayer structures, a coating for solar cells (Hamakawa, 1982) and as a connection material for Very Large Scale Integrated (VLSI) devices.

Despite almost two decades of study, very little can be concluded about the electronic properties of these materials. Even the basic theory of conduction is still in dispute. However it is necessary to make some assumptions about the material properties preceeding the study. Firstly, it is assumed that there are band tails in the energy gap of a-Si:H, arising from the disordered structure. Band-tails are essentially extensions of the conduction and valence bands into the energy gap, however they do not exhibit extended-state conduction. Instead they conduct by a hopping process which greatly reduces the mobility of these states. Several structural models have been proposed for a-Si:H, as can be seen in Figure 1.1. They all include band-tail states, and thus there is some concensus on their existence.

Secondly, it is necessary to assume some typical range for the electron and hole mobilities in a-Si:H. A range of $\sim$1-10cm^2/V.sec. for μ_n and 10^{-4}-10^{-3}cm^2/V.sec. for μ_p has been generally assumed (Mott and Davis, 1979). Comparing this electron mobility with that of c-Si, which is on the order of 1000cm^2/V.sec., we can see that the disordered structure again markedly affects the fundamental electronic properties.

Thirdly, we expect that there will be no change in the value of the effective density of states (DOS) at the conduction band edge or at the valence band edge as we compare the films with each other. Because of this assumption, any change in properties must be related to changes in the distribution and density of localized states in the gap. Of course, many other assumptions will be made in this thesis, but they will not be as basic as the aforementioned three.

Despite the structural disorder of a-Si:H films the gap states still exhibit the same processes that they would in c-Si. There are eight basic processes of relaxation and excitation that describe the influence that the gap states have on the electronic properties of materials, six of which are shown in Figure 1.2. The other two processes are not included because they infer a process of photoluminescence, which we have not observed. If the electron absorbs a photon, phonon or a number of phonons it will rise to a higher energy level, as shown in transitions 1, 3 and 5. If the electron emits a photon, phonon or a number of phonons it will fall to a lower energy level, as shown in transitions 2, 4 and 6. These six transitions are the focus of much of this thesis.

In the following four chapters we shall present our analysis of our observations. In chapter two we review the theories of both the dark conductivity and the photoconductivity processes which have been put forward to explain the electronic behaviour of a-Si:H films. In chapter three we discuss the transition from the amorphous to microcrystalline phase which has been achieved by changing the magnetic field in our microwave plasma system. In chapter four we present our experimental results on the photoconductivity of a-Si:H films, and our new model describing the relationship between the photoconductivity and the light intensity. The conclusions of our study are given in chapter five. Details of the experimental methods and equipment are given in the Appendix.

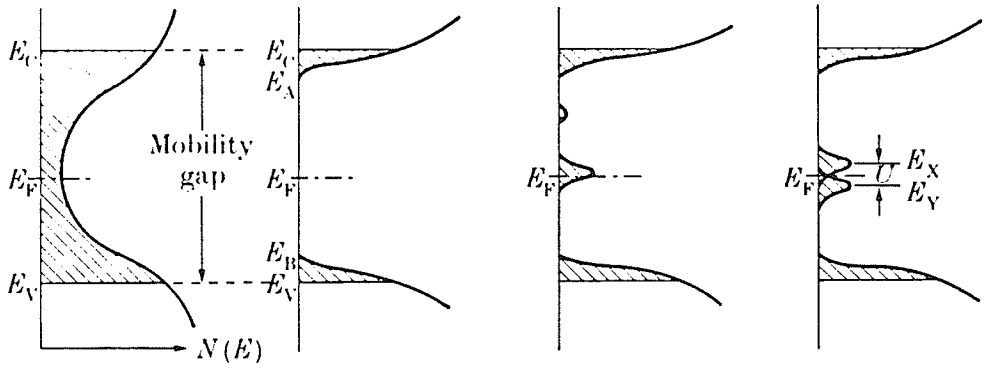

FIGURE 1.1 Various forms proposed for the density of states in amorphous semiconductors. Localized states are shown shaded. (a) Overlapping conduction and valence band tails as proposed by Cohen *et al.* (1969), the CFO model; (b) a real gap in the density of states, suggested here as being appropriate for a continuous random network without defects; (c) the same as (b) but with a partially compensated band of defect levels; (d) the same as (b) but with overlapping bands of donor (E_Y) and acceptor (E_X) levels arising from the same defect. (The model for chalcogenides, which involves two-electron energy levels, is not shown in this diagram.) **(Mott and Davis, 1979)**

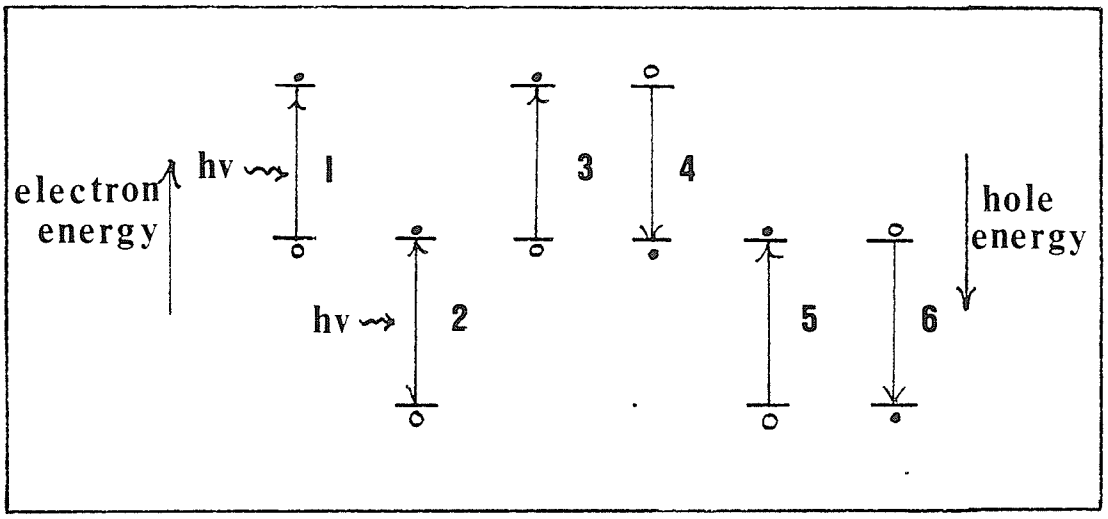

FIGURE 1.2. Six Basic Electron Transitions.

1- Optical excitation to a higher energy level.

2- Optical excitation from a lower energy level.

3- Thermal excitation to a higher energy level.

4- Electron capture.

5- Thermal excitation from a lower energy level.

6- Hole capture

(• -electron; ∘ -hole)

CHAPTER 2: ELECTRONIC CONDUCTION IN a-Si:H FILMS

In this chapter we summarize much of the recent literature on steady state electric conductivity and review the current explanations for dark conductivity and photoconductivity phenomena. In Section 2.1, on dark conductivity, we present the principles of extended-state and hopping conduction and discuss the typical behaviour of the dark conductivity as a function of temperature. In Section 2.2 we discuss photoconductivity and four important processes in a-Si:H films, namely; (1) absorption; (2) thermalization; (3) quantum efficiency; and (4) recombination. Following this we shall discuss the effects of temperature, light intensity, photon energy, and electric field on the photoconductivity.

2.1 Dark Condition

The dark current-voltage (I-V) characteristics of a-Si:H films are mainly associated with two different conduction mechanisms; namely the extended-state conduction and hopping conduction. Extended-state conduction occurs for electrons above the conduction band edge or holes below the valence band edge in a manner analogous to that in crystalline materials. Hopping conduction may occur in the band tails in the intermediate temperature range (270-230K) but it is, in general, only dominant at low temperatures when it occurs at the Fermi level. These two conduction mechanisms will be discussed in the next section, after which typical results and interpretations of dark conductivity in a-Si:H films will be briefly reviewed.

2.1.1. Extended State Conduction

As in crystalline materials, each electron can be described in terms of a wave function which is a solution to the Schrodinger equation. The wave functions in disordered materials, however, are not the same as those in crystalline materials (Mott and Davis, 1979) and they have not been solved to date. An important difference between crystalline and amorphous silicon is the possibility of a minimum metallic conductivity in the amorphous material arising from its disordered structure. The minimum metallic conductivity causes a finite conductivity to exist even at absolute zero. The theory of the minimum metallic conductivity and the correct expression to describe it are beyond the scope of this thesis.

2.1.2 Hopping Conduction

When the Fermi energy lies in or below localized states there is the possibility that the conduction process can be described by hopping, in which an electron tunnels among states that lie within a few kT of each other. We discuss two types of hopping, specifically nearest neighbour and variable range hopping.

For nearest neighbor hopping, which occurs for strong localization, the number of electrons jumping a distance R_j in the direction of an applied field consists of: (a) the number of electrons per unit volume within a range kT of the Fermi level, namely $2n(E_F)kT$; and (b) the difference of the hopping probabilities in the two directions, which is

$$v_{ph}\exp\left\{-2\alpha R_j - \frac{W \mp qR_jE}{kT}\right\} \tag{2.1}$$

where E is the applied field. The current is now found by multiplying by q and R_j, and is thus

$$J = 2qR_jkTN(E_F)v_{ph}\exp\left\{-2\alpha R_j - \frac{W}{kT}\right\} \quad \mathrm{Sinh}\left\{\frac{qR_jE}{kT}\right\} \tag{2.2}$$

For weak fields, such that $qR_jE \ll kT$, the current may be expressed more simply as

$$J = 2q^2R_j^2Ev_{ph}N(E_F)\exp\left\{-2\alpha R_j - \frac{W}{kT}\right\} \tag{2.3}$$

Another aspect of this conduction is called variable range hopping, which occurs at low temperatures for the condition that the thermal energy of

hopping can only be satisfied when the electron hops some distance, further than a nearest neighbour. The conduction depends on T as exp $(-B/T^{1/4})$, or, in two dimensions, as exp $(-B/T^{1/3})$, in which B is given by

$$B = 1.66 \left\{ \frac{\lambda^3}{KN(E_F)} \right\}^{1/4} \tag{2.4}$$

where λ is the decay rate of the localized wave functions and $N(E_F)$ is the density of localized states at the Fermi level. Thus, the conductivity can be written as

$$\sigma = q^2 N(E_F) \bar{R}_j^2 \exp \left\{ -B/_T{}^{1/4} \right\} \tag{2.5}$$

where $\bar{R}_j$ is the mean value of the jumping distance. For this type of hopping the conduction for moderate fields becomes (Mott and Davis, 1979).

$$\sigma = q^2 N(E_F) R_j^{-2} \exp \left\{ -B/_T{}^{1/4} \right\} \exp \left\{ \frac{qE\gamma R_j}{kT} \right\} \tag{2.6}$$

where γ is a constant, which is about 0.17, and R_j is the low field hopping distance. Later, we shall discuss how these two mechanisms interact to yield a dark conductivity-temperature characteristic.

For dark conduction the conductivity is expected to consist of three components, which are: (a) a component due to electrons at the mobility edge,

$$\sigma = \sigma_1 \exp \left\{ \frac{-(E_c - E_F)}{kT} \right\} \tag{2.7}$$

(b) a component due to electrons in the conduction band tail,

$$\sigma = q\mu N_c \exp \left\{ \frac{-(E_A - E_F)}{kT} \right\} \tag{2.8}$$

where N_c is the effective density of states in the conduction band, $E_c - E_A$ is the width of the conduction band tails, and μ is the hopping mobility. Two of these terms are expressed below.

$$N_c = \int_o^{kT} N(E)\, dE \tag{2.9}$$

$$\mu = V_{ph} \frac{qa^2}{kT} \exp\left\{\frac{-W}{kT}\right\} \tag{2.10}$$

Finally, (c) a component due to conduction at the Fermi level, which has already been given by Equation (2.5).

2.1.3 General Observations

Generally, the conductivity as a function of temperature consists of the aforementioned three components, and can be expressed as

$$\sigma_d = \sigma_1 \exp\left\{\frac{-E_1}{kT}\right\} + \sigma_2 \exp\left\{\frac{-E_2}{kT}\right\} + \sigma_3 \exp\left\{-B/T^{1/4}\right\} \tag{2.11}$$

where $\sigma_1 = q\mu_c N_c \exp(\gamma'/R)$, μ_c is the mobility in the extended states, N_c is their effective density, and γ' is the energy gap temperature coefficient. Equation (2.11) adequately describes the temperature dependence of the conductivity. In general, the middle term is negligibly small. At high temperatures the first term is dominant, and so the activation energy is $E_1 = E_c - E_{Fo}$, which determines the approximate position of the Fermi level. Furthermore, from σ_1 we can determine the relative change in μ_n and γ' for different films. At low temperatures the third term becomes dominant. Then, from B, we can calculate the density of states at the Fermi level with an assumed value for λ.

A typical plot of μ_n and σ_d as a function of temperature is shown in Figure 2.1. The drift mobility is expressed as (Mott and Davis, 1979).

$$\mu_d = \mu_o \exp\left\{-E_a/kT\right\} \tag{2.12}$$

where E_a is 0.19eV for $T \geq 240^\circ K$ and 0.09eV for $T < 240^\circ K$. The kink in the drift mobility plot is a result of the change from extended state conduction to band tail hopping. The extended state activation energy arises from trapping in the shallow localized states below E_c, whereas the band tail hopping activation energy is due to the mechanics of the hopping process (Mott and Davis, 1979). The conductivity curve does not show a kink at this temperature, indicating that the temperature dependence of the mobility is not the dominant mechanism causing the temperature dependence of the conductivity. Instead, the conductivity temperature dependence is dominated by the Fermi level position for temperatures above 220 K, indicating that the carrier concentration dominates the high temperature conductivity behaviour.

In conclusion, most of the conductivity mechanisms are still under discussion. Interpretations of many of the parameters are at odds with the experimental evidence. A typical example of this disagreement occurs for the conductivity prefactor σ_1. The value of σ_1 is expected to remain well-bounded in theory, between 200 and 400 S/cm (Mott and Davis, 1979), however it shows large changes in its value from sample to sample. If the theory is correct, this change implies that the mobility, effective

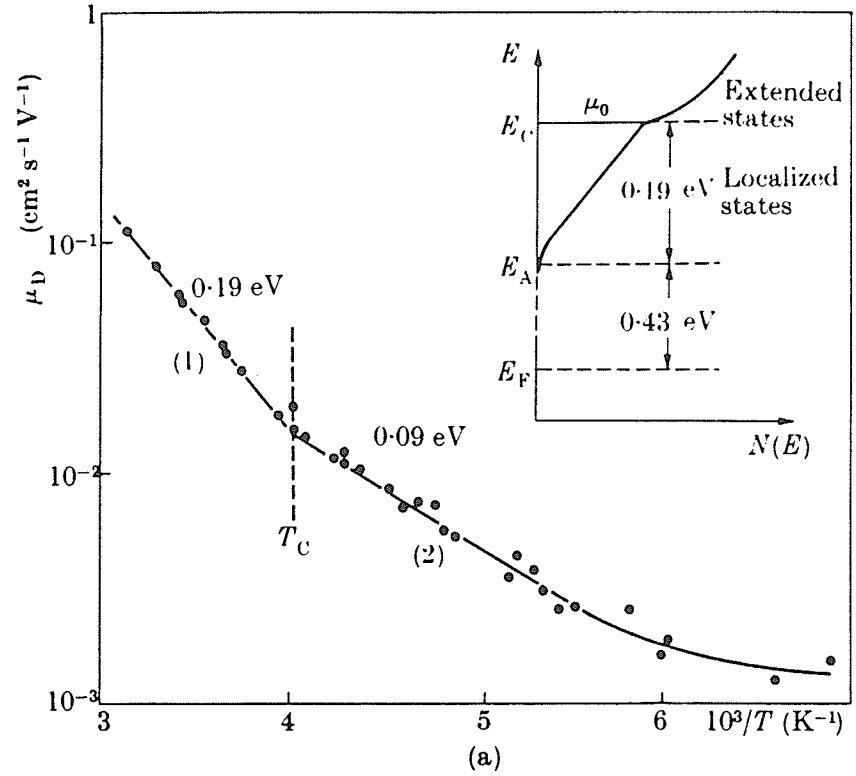

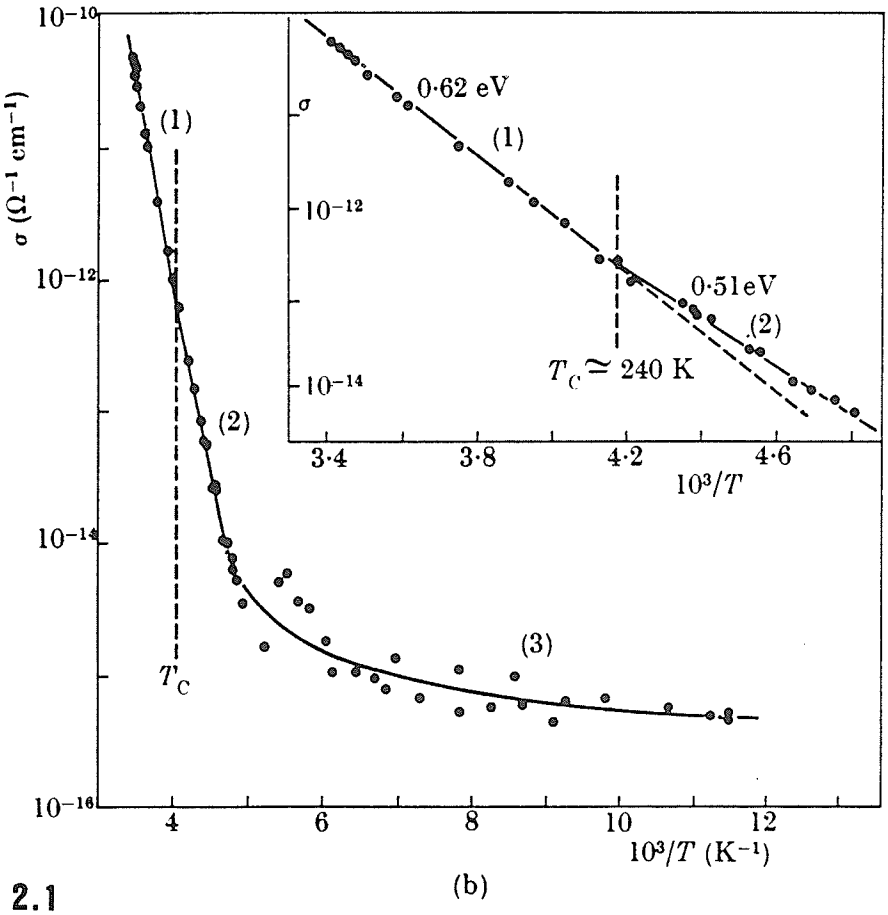

FIGURE 2.1

Temperature dependence of (a) electron drift mobility μ_D, (b) conductivity σ in a glow-discharge film of silicon deposited at 500 K. (From Le Comber and Spear 1970.)

density of states in the conduction band, or the band gap temperature coefficient changes from sample to sample by large amounts. One attempt to explain the variations in σ_1 suggests that by allowing the mobility edge to fluctuate in space due to the presence of long-range disorder, and by viewing the film as a network of cells connected in one of several possible ways, the spread of the prefactor over four orders of magnitude can be well accounted for (Overhof and Beyer, 1981). More study is needed to successfully interpret the dark conductivity results.

2.2 Photoconduction

Photoconductivity (PC) is defined as the excess conductivity produced by optical excitation. There are in general two mechanisms by which this excess conductivity may take place (Bube, 1960). First, the optical excitation may increase the density of conducting carriers by exciting electrons and holes into conducting states. This is the dominant process in a-Si:H, as it is in most materials. Secondly, the optical excitation may cause a reduction in the potential barriers for conduction in the film, either due to minority or majority carrier space charge. This possibility is usually not discussed, therefore we do not discuss it either.

To discuss the photoconductivity (PC) of a-Si:H films we shall consider the following topics as forming a basis for future discussions. These topics are absorption, thermalization, quantum efficiency and

electron lifetime. Upon this basis we shall then discuss the effects of temperature, photon energy, light intensity and electric field, and analyze typical behaviour for a-Si:H films.

Considering that the photocurrent is mainly due to the flow of electrons (with the contribution of holes neglected), the photocurrent is given by (Mott and Davis, 1979),

$$J_{ph} = q\mu_n EG'(1-R)\left\{\frac{1-\exp(-\alpha d)}{d}\right\}\tau_n \eta \qquad (2.13)$$

where q is the electron charge (1.6×10^{-19}C/el.), μ_n is the electron mobility (cm^2/V.sec), E is the applied field (V/cm), α is the absorption coefficient (cm^{-1}), d is the sample thickness (cm), η is the quantum efficiency and τ_n is the free electron lifetime (sec).

2.2.1 Absorption

For the photon energy range used for this investigation ($E_g/2 \leq h\nu \leq 2Eg$), the absorption occurs when an electron is excited from its initial state, either in the valence band or in a localized gap state, to its final state, either in the conduction band or in a localized gap state. For this range of photon energies three separate regimes can be defined. The first regime exists for $0.6 < h\nu < 1.4$eV. Since a-Si:H has, in general, Eg=1.7ev, we immediately recognize that the transitions must include the localized gap states. There are three possible transitions namely: (1) the valence band to a localized gap state, (2) a localized gap state below the midgap to a state above midgap, and 3/a

gap state to the conduction band. The absorption spectrum will provide some information on the distribution of localized states in the gap, because the optical transition matrix is proportional to the density of the initial and final states. Several investigators have calculated the gap state distribution based on the absorption spectra (Abeles et al, 1980; Cody et al, 1980; Loveland et al, 1973; Moddel et al, 1980; Moustakas 1980; Pankove et al, 1980). The second regime of absorption occurs in the range $1.4eV \leq hv \leq 2.4eV$. This regime is characterized by a steady increase in the absorption coefficient from a relatively low value (10/cm) units at hv=1.4eV to a high value (10^5/cm). This regime is called the Urbach edge and the relation of α to hv is expressed as

$$\alpha(hv)hv \sim (hv-E_o)^{1/2} \qquad (2.14)$$

where E_o is a fitting parameter, which is generally referred to as the optical gap. Generally the characteristic energy of this line has a value between 0.05eV and 0.09eV for a-Si:H (Abeles et al, 1980; Cody et al, 1980; Crandall, 1980; Mott and Davis, 1979). The presence of this region in the absorption spectra is generally considered as indicative of internal field broadening of the band edge excitonic absorption (LeComber and Mort, 1971). The third regime occurs in the range of $2.4eV < hv < 3.0eV$. In this range the absorption coefficient is essentially constant. Theoretically, the constant absorption is a consequence of the very short mean free path for electrons in a-Si:H ($kL \sim 1$). This causes a relaxation of the k- selection process for optical absorption (Mott and Davis, 1979), which means that more optical transitions are allowed in the amorphous state than in the crystalline state. All three regions of the absorption spectra are shown in Figure 2.2.

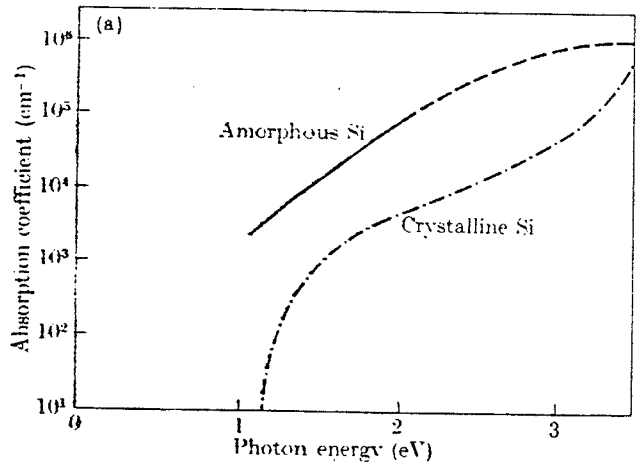

a

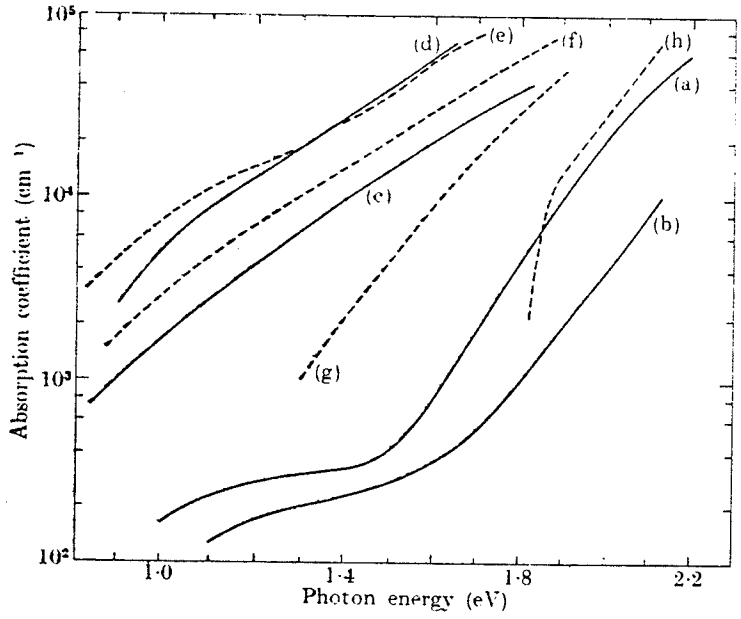

Optical absorption edges in amorphous silicon prepared by different methods: (a) glow-discharge films deposited from 500 to 600 K; (b) glow-discharge films deposited at ~300 K; (c) and (f) sputtered films; (d) and (e) evaporated films; (g) annealed sputtered film; (h) 'extrapolated' edge (Brodsky, Kaplan, and Ziegler 1972, see § 7.3). (From Loveland *et al.* 1973/74.)

b

FIGURE 2.2 The absorption spectra of a-Si films:

a- a comparison of the amorphous and crystalline phases;

b- detailed values at low photon energies. (Mott and Davis, 1979).

Figure 2.3 illustrates that the absorption process can be visualized as occurring in the Coulomb well of the photoexcited hole. The electron and hole will exert a Coulomb force on each other and the electron will move by diffusion in this well. The hole is immobile in relation to the electron (Carasco and Spear, 1983).

2.2.2 Thermalization

Immediately after photoexcitation the electron will be at an energy level ΔE in relation to the conduction band edge, where

$$\Delta E = h\nu = E_g \quad \text{for } h\nu > E_g \tag{2.15}$$
$$\Delta E = E_g - E_i - h\nu \quad \text{for } h\nu < E_g$$

where E_i signifies the energy level of the initial state in the transition. After the transition the electron will exchange energy with the lattice, thereby proceeding to a new energy level where it moves in thermal equilibrium with the lattice. This movement of the electron to an equilibrium energy level is diffusive in nature, and is called thermalization (Carasco and Spear, 1983).

Two parameters which characterize this thermalization process are the thermalization distance, which is the final separation of the electron and hole, and the thermalization time, t_T. By assuming that the electron loses one phonon quantum, $\hbar w_{ph}$, per unit time, $^1/w$, and that the hole is immobile, the electron will thermalize by diffusion to a thermalization

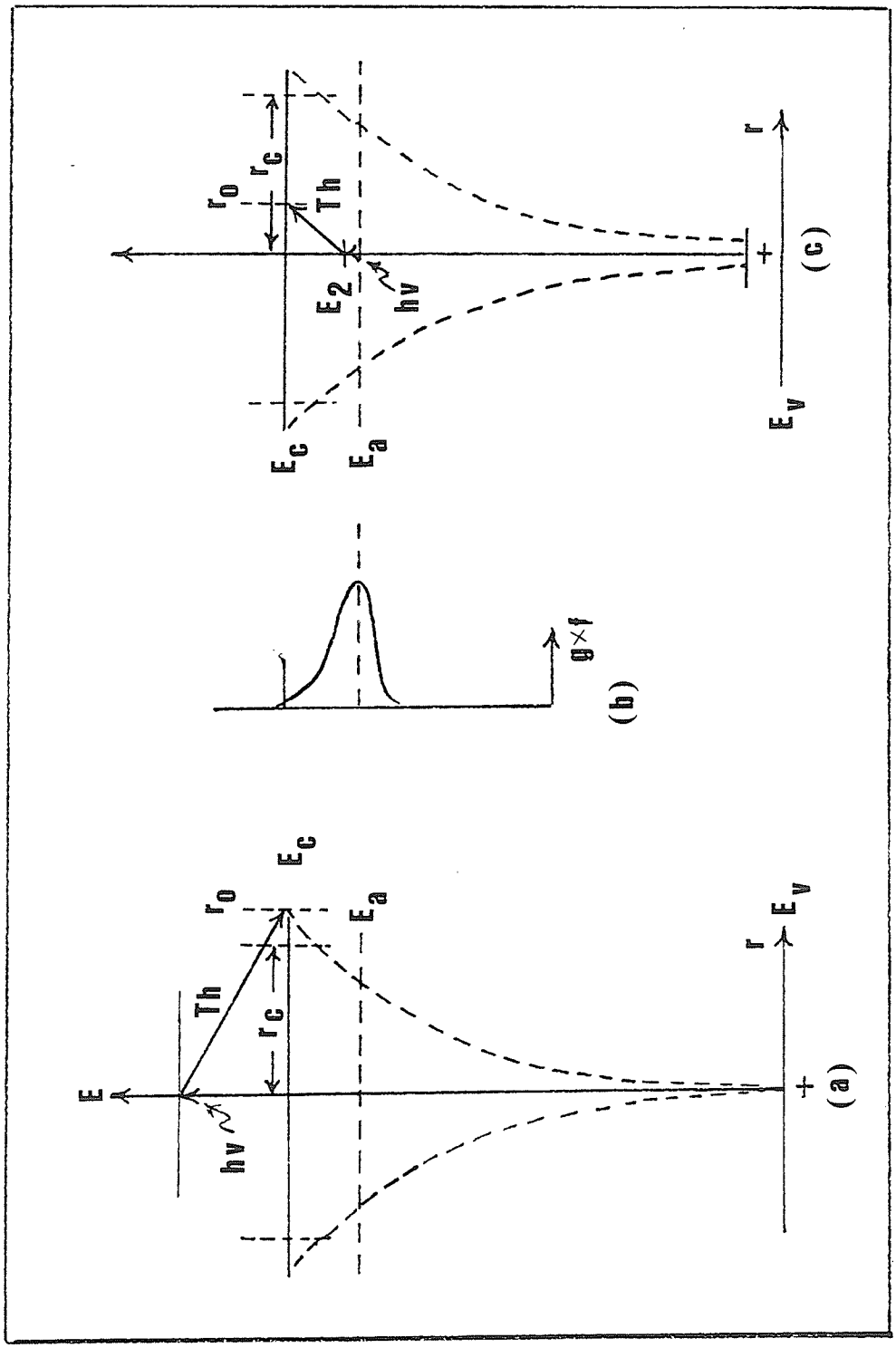

FIGURE 2.3 The Absorption and Thermalization processes for electrons excited into (a) the extended states, and (c) the localized states; (b) Energy distribution of electrons after thermalization (Th). (Carasco and Spear, 1983).

distance, r_o, given by (Mott and Davis, 1979)

$$r_o = \left\{ \frac{\Delta E + \left(\frac{q^2}{Er_o D}\right)}{\hbar w_{ph}^2} \right\}^{1/2} \qquad (2.16)$$

where D is the diffusion coefficient and E is the permittivity of a-Si:H. Alternatively, the relative value of r_o can be found from (Knights and Davis, 1974)

$$r_o \propto \left\{ \hbar w_{ph} - E_g - \frac{q^2}{4\pi E r_o} \right\}^{1/2} \qquad (2.17)$$

These equations simply imply that the thermalization distance is dependent on temperature through $\hbar w_{ph}$ and D, and on photon energy through ΔE. To date there is no one theoretical expression which can accurately relate a specific photon energy to a specific thermalization distance.

The thermalization rate has been reported to be~0.1eV/psec (Vardeny and Tauc, 1980), and so the thermalization time will be on the order of a picosecond. These investigators have also reported that the thermalization time and distance are rather weakly dependent on photon energy in the range $1.85eV<hv<2.3eV$. The thermalization process is generally ignored for steady-state PC studies, but may have important implications for the low temperature photoconductivity (Hoheisel et al, 1983; Misra et al, 1983).

2.2.3 Quantum Efficiency

In a-Si:H films, the absorption of a photon will not necessarily lead to two free carriers, even with hv>Eg. After thermalization both the electron and hole may experience geminate recombination, in which the same electron and hole that were photoexcited recombine at about the same time. The probability of geminate recombination is directly related to the potential energy of the hole's coulomb well and the thermalization distance, as shown in Figure 2.3. The spatial extent of the coulomb field of the hole, r_c , can be estimated by equating the coulomb potential to the average thermal energy, which yields

$$r_c(T) = \frac{q^2}{(4\pi\varepsilon EKT)} \qquad (2.18)$$

For a-Si:H films, for which the dielectric constant is 12 E_o, $r_c \doteq 50\text{Å}$ at room temperature. There are three possibilities: (i), if $r_o \geq 4r_c$, the excited electron and hole will be considered to be free, leading to a quantum efficiency (Q.E.) of 1; (ii), if $r_o < r_c$, but there is a preference for ionization, the value of Q.E. can still be unity; (iii) if $r_o < r_c$, and there is a preference for recombination, the Q.E. will drop from unity and hence the photocurrent will decrease.

A more analytical approach is due to Onsager (1983), who has derived the quantum efficiency (Q.E.) as a function of applied field. His analytical expression is given by (Adler et al, 1980)

$$\eta(E,T,r_o) = \eta_o \exp\left\{\frac{-r_c}{r_o}\right\}\left\{1 + \frac{1}{2}\left(\frac{q}{KT}\right)(r_c E) + \ldots\right\} \qquad (2.19)$$

where N_o is the quantum efficienty of the initial process. This equation may be expressed more generally as (Carasco and Spear, 1983).

$$\eta(E,T,r_o) = n_o \Omega(E,T,r_o) \qquad (2.20)$$

Where $\Omega(E,T,r_o)$ is an expression for the probability for the electrons to escape the attraction of a Coulomb well. It can be seen that for $r_o < r_c$ the Q.E. is reduced considerably, and it becomes increased only when the applied field reaches or becomes higher than the critical field value $E=kT/qr_c$. The theoretical relationship between Q.E. and applied field is illustrated in Figure 2.4.

From the previous discussion we can conclude that there are three necessary characteristics when geminate recombination becomes important (Adler et al, 1980): (1) a rapidly increasing photo conductive yield saturating at $\eta=1$ as the photon energy of the light increases; (2) a decreasing activation energy for the photoconductivity as the photon energy increases, based on the expression for the activation energy

$$E = q/(4\pi\varepsilon r_o) \qquad (2.21)$$

and, (3) an increase in yield at applied fields in excess of 10^4V/cm at room temperature, or 10^3 V/cm at a temperature of 100°K.

For transitions into localized states we need to account for several additional complications (Carasco and Spear, 1983). First, the diffusive separation achieved during thermalization will be appreciably smaller for an electron in the tail states as compared to that in the conduction band. At room temperature the hopping mobility in the tail states is~ 50 to 100

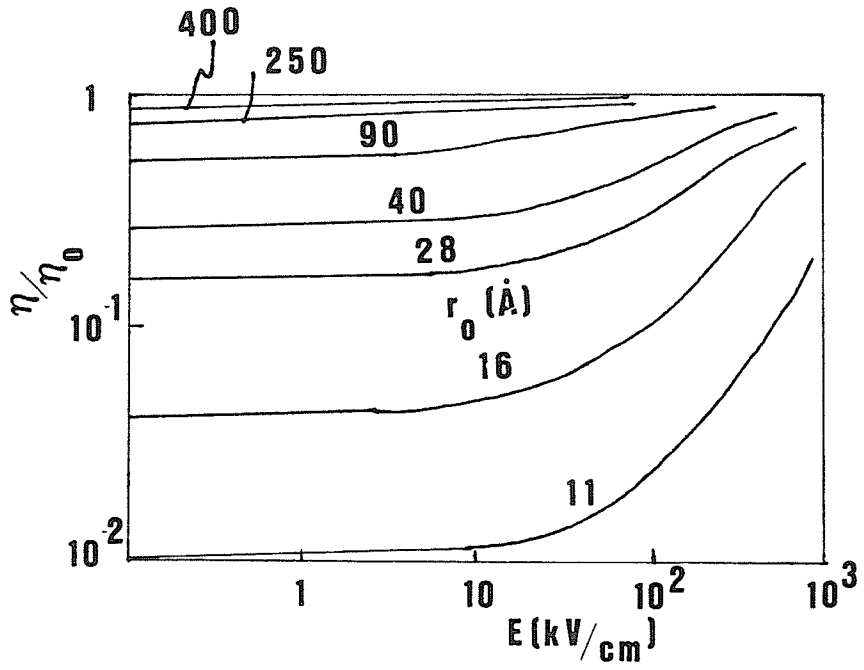

FIGURE 2.4 The Onsager function η/η_0 plotted against the applied electric field(E) for the indicated values of the thermalization distance, r_0(Å). The calculations are for a-Si at room temperature. (Carasco and Spear, 1983).

times smaller than the extended state mobility. Secondly, the electron distribution during thermalization, shown in Figure 2.3(b), is now produced well within the coulomb well. If we assume that all the electrons which are thermalized into the localized states experience geminate recombination, the expression for Q.E. refers only to those electrons in the extended states. Therefore the Q.E. for transitions into the bandtails is (Carasco and Spear, 1983)

$$\eta \propto \frac{g(E_c)}{g(E_2)} \exp\left\{\frac{-(E_c - E_c)}{KT}\right\} \Omega_\perp(E,T,r_o) \qquad (2.22)$$

where E_2 is the energy of the gap state involved in the optical transition and $g(E_2)$ refers to the density of states at that level. Based on this equation we should observe a rapid decrease in PC for transitions into the localized states as compared to the conduction band (Moddel et al, 1980; Crandall, 1980). The expected photon energy dependence of the Q.E. is rarely observed and provides a further complication to the interpretation of the PC (Crandall, 1984).

2.2.4 Lifetime

The final variable in the basic equation for photoconductivity is the free electron lifetime, which is defined as the time the electron spends in the conducting state before it recombines with a hole. The lifetime of an electron ranges from 10^{-12} sec. to 10^{-2} sec. for a-Si:H films, and is related to the density of states that can capture electrons and the probability of capture by those states. Recombination can be

described in many ways, including the terms bimolecular, monomolecular, ballistic and diffusive. Bimolecular recombination refers to the recombination process in which the free hole and free electron recombine simultaneously. For a-Si:H films this term is used whenever the PC intensity dependence exhibits a square-root behaviour. The probability of band-to-band transitions is negligibly small because of the high density of localized states in the gap. Monomolecular recombination refers to the transition in which either the electron or hole is already trapped before the occurrence of their recombination. In a-Si:H films monomolecular recombination is the dominant transition.

The terms ballistic and diffusive recombination refer to the relative electron scattering length. Ballistic capture is applied to materials in which the scattering length is larger than the capture radius. Diffusive capture is applied to low mobility materials for which such an inequality does not hold (Street, 1984). An important difference between these two capture processes is that the bottleneck for ballistic capture is the ability of the electron to lose energy, whereas for diffusive capture it is the ability of the electron to diffuse to the recombination centre (Crandall, 1984). By assuming that the lifetime is governed by a ballistic, monomolecular process, the lifetime may be written as (Bube, 1960)

$$\tau_n = \left\{ (v\sigma_n) p_R \right\}^{-1}$$

where v is the microscopic thermal velocity ($10^7 cm^2/sec$ at T = 300K), σ_n is the capture cross-section and p_R is the density of recombination centres. This equation implies that only one type of centre is participating in the recombination traffic. In the following section we shall discuss the capture cross-section, the microscopic velocity and the density of recombination centers.

Capture Cross-Section: The capture process in any material is generally coulombic in nature, and therefore we may classify states according to their charge, such as positive, neutral, negative, doubly negative, etc.. For the capture of electrons these states could also be classified as attractive, neutral, repulsive, doubly repulsive, etc.. These centres are shown schematically in Figure 2.5. The size of the capture cross-section for each of these states is difficult to calculate. However, for the attractive centre a simple method is often used. By setting the thermal energy, kT, equal to the coulomb attractive energy, the radius of the capture cross-section can be expressed as (Bube, 1960)

$$R = \frac{q^2}{(4\pi \epsilon kT)} \tag{2.24}$$

and, therefore, the capture cross-section is

$$\sigma_n = \pi r^2 = \frac{q^4}{(16\pi(\epsilon kT)^2)} \tag{2.25}$$

This is only an approximate expression, but it indicates the type of temperature dependence to be expected. For neutral and repulsive centres the calculation becomes more complex. Neutral centres are sometimes identified as being weakly dependent on temperature (Bube, 1960), whereas repulsive centres can be weakly dependent or strongly dependent, depending

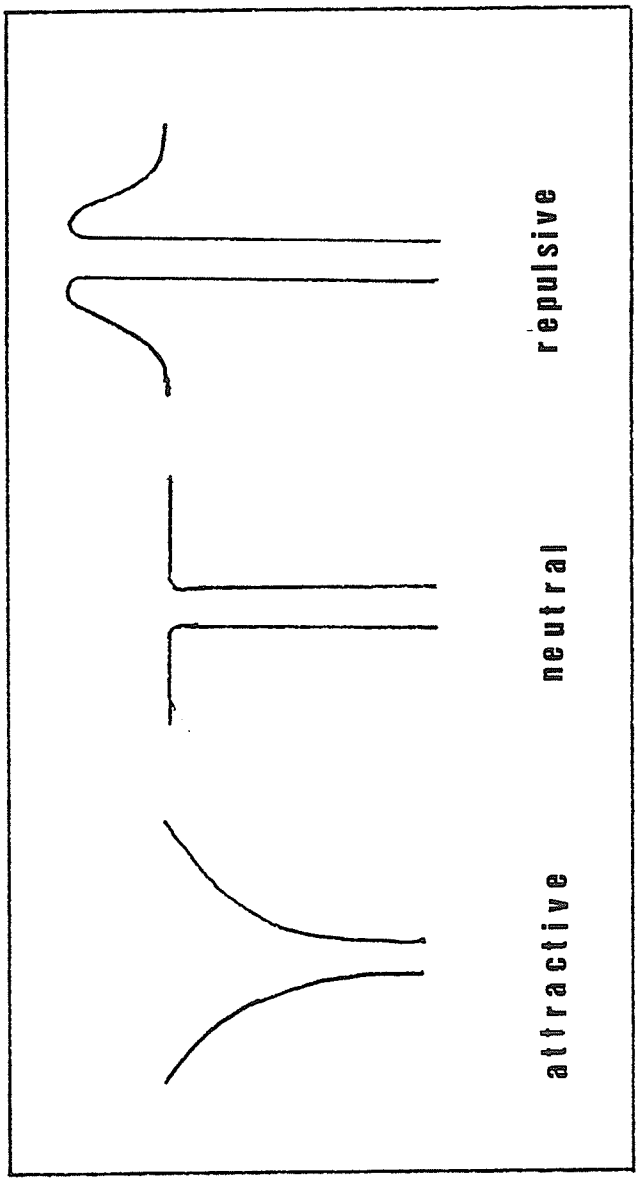

FIGURE 2.5 The coulomb field of three types of states.

on the possibility of tunneling through the barrier (Milnes, 1973). In general, the capture cross-sections are within the range from $10^{-12}cm^2$ to $10^{-22}cm^2$, with the largest value for the attractive centres and the smallest value for the repulsive centres (Bube, 1960).

In a-Si:H films the capture cross-sections have been measured, and generally lie in the range $10^{-21}$to $10^{-14}cm^2$ (Persans, 1982; Wronski and Daniel, 1981; Street, 1984; Vanier et al, 1981). For the traps located at levels from the midgap to 0.35eV below the conduction band the capture cross-sections are generally constant ($10^{-15}cm^2$), whereas smaller sizes are found for those states below midgap (Vanier et al, 1981; Wronski and Daniel, 1981). Presently there is evidence that the dangling bonds in a-Si:H films may produce gap states at two or three distinct levels, including a neutral centre or a doubly repulsive center (Crandall, 1984).

The temperature dependence of these capture cross-sections have not been determined. A strong temperature dependence of $T^{-3}$for attractive centres and $T^{-1.5}$for neutral centres has been proposed (Street, 1984), in which the effects of the minimum metallic conductivity and the trap-controlled mobility are included. This study was performed specifically for a-Si:H films. Another investigator merely speculates that there may be a temperature dependence (Persans, 1982).

Another possible recombination process is the tunneling of an electron from the tail state to a defect (Street, 1984; Dersch et al, 1983). The total cross-section for the defect can then be written as (Street, 1984)

$$\sigma_n = \sigma_p + \sum_{\substack{\text{tail} \\ \text{states}}} \sigma_T \bar{P} \tag{2.26}$$

If we assume that $\sigma_D \doteq \sigma_T$, and that capture is ballistic, then

$$\sigma = \sigma_D (1 + \bar{P}) \tag{2.27}$$

and so we can think of the tunneling process as adding an enhancement factor equal to $(1+\bar{P})$. The factor $\bar{P}$ is the tunneling probability for a tail state at E below the mobility edge, and is found by integrating over the energy E, and the distance from the tail state to the defect R. This yields (Street, 1984)

$$\bar{P} = \frac{3}{4} N_c R_o^3 k T_c \left\{ (T_c/T)^3 + (T_c/T)^2 + (T_c/T) + 1 \right\} \tag{2.28}$$

The tunneling contributes an increasing amount as the temperature is reduced, and becomes especially important at low temperatures.

Microscopic Velocity: The value of v is simply determined by setting the average thermal energy equal to the average kinetic energy, which yields

$$v = \left[\frac{(3kT)}{m} \right]^{1/2} \tag{2.29}$$

At room temperature $v = 10^7 cm^2/sec$.

Recombination Centre Density: There are two electron transitions which are important for a recombination centre. These are the rate of electron capture (R_n) and the rate of hole capture (R_p).

In the steady-state these rates are equal and so $R_n = R_p$ which means that (Bube, 1960)

$$R_n = np_R v\sigma_n = R_p = pn_R v\sigma_p \tag{2.30}$$

where n_R (p_R) are the densities of filled (empty) recombination centres and n(p) are the densities of free electrons (holes). The total density of centres is $N_R = n_R + p_R$. Depending on the ratio of σ_n to σ_p and the ratio of n to p the recombination centre densities may be found by these two equations. Specifically (Rose, 1963)

$$p_R = N_R \frac{(\sigma_p p)}{(\sigma_p p + \sigma_n n)}$$

and (2.31)

$$n_R = N_R \frac{(\sigma_n n)}{(\sigma_p p + \sigma_n n)}$$

The analysis which is necessary for the complete determination of n_R and p_R is difficult to use and does not always provide physical insight into the recombination behaviour. However, several analysis methods for finding n_R and p_R have been put forward to date (Shockley and Read; 1956; Rose, 1963; Simmons and Taylor, 1972, 1974; Hack et al, 1984). Usually the analysis involves the kinetic and thermal equations necessary for recombination centres and traps, respectively, and the demarcation or

equality levels, which separate the trapping and recombination centres. As the light intensity increases or the temperature decreases the demarcation levels move toward the band edges, thus changing traps into recombination centres. This is the essential feature of all these models - using the movement of these levels to adjust the values of n_R and p_R to fit the experimental data.

Some investigators include the possibility of localized state to localized state transitions (Arnoldussen et al, 1972; Simmins and Taylor, 1974), however no one includes the possibility of recombination by tunneling at low temperatures. Therefore, there is a need for further modelling to adequately describe the PC of a-Si:H films.

2.2.5 Observed Photoconductivities

In our experimental work we used the temperature, light intensity, photon energy and electric field as variables and observed their effects on photoconductivity. In the following we shall present their effects, as observed in a-Si:H films, and their relevant explanations. First we shall present the temperature dependence of the photoconductivity (PC), including a description of the two PC maxima and the low temperature behaviour. Then we go to the meaning underlying the photon intensity dependence, followed by a discussion of the effects of photon energy and electric field.

The Effects of Temperature

Typical temperature-photoconductivity characteristics are shown in Figure 2.6. There are five regimes possible, although often only three are observed (Mott and Davis, 1979). These five regimes can be separated into four distinct features, these being: (1) the high temperature PC maximum; (2) the decrease of PC as temperature decreases; (3) the low temperature PC maximum; and (4) the low temperature saturation of PC. We discuss these features in this order.

The two sides of the PC maximum, regimes 1 and 2, can be roughly classified by the relation between the photoexcited and dark electron populations, although this is not always completely correct. In regime 1 $n_o > n_{ph}$ and the thermal equilibrium electron density, n_o, controls the lifetime. Often the photocurrent decreases as the temperature is increased, which indicates that the lifetime for the photoexcited electrons is not constant. One explanation (Mott and Davis, 1979) assumes that there are two sets of states in the gap, with E_y below the midgap and E_A above the midgap. As temperature increases in regime 1 more holes are available to move to the E_y states, thus increasing p_R and causing the activation energy $E = E_{Fo}-E_y$. If we assume that the mobility is activated at an energy$\sim$0.2eV, the commonly observed PC activation energy of 0.2eV indicates that the energy level of E_y is$\sim$0.4eV below E_{Fo}. The observed activation energy of the PC should change as the Fermi level shifts from sample to sample.

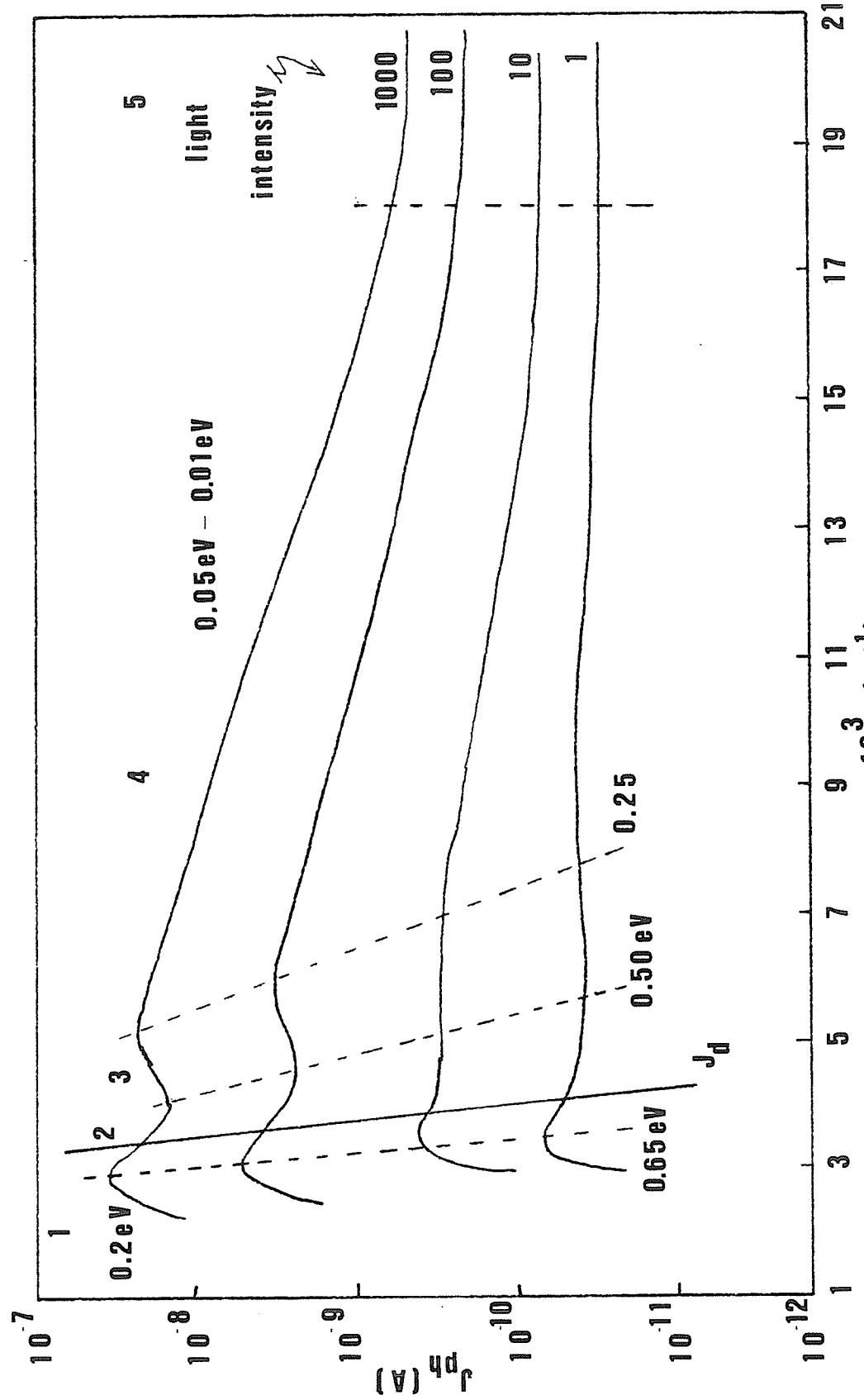

FIGURE 2.6. The effect of temperature on photoconductivity. Typical activation energies and relative light intensities are shown.

Another theory for regime 1 also assumes a two-state model for the gap state density distribution, in which E_1 is near the conduction band tails, $E_1 = E_c - 0.1eV$, and E_2 is below the midgap, E_2 0.4eV (Shirafuji et al, 1985). If the dominant recombination step is due to the movement of electrons from E_1 to E_2, then

$$J_{ph} \sim G\mu \exp \left\{ \frac{(E_{Fo}-E_2)}{KT} - \frac{(E_c - E_1)}{KT} \right\} \tag{2.32}$$

however if the dominant process is the transition from the conduction band edge to E_2 then

$$J_{ph} \sim G\mu \exp \left\{ \frac{E_{Fo} - E_2}{KT} \right\} \tag{2.33}$$

Another two state model proposed by Simmons and Taylor (1974) give J_{ph} in regime 1 as

$$J_{ph} = q\mu E \left\{ \frac{G}{\sqrt{5} n N_t} \right\} \exp \left\{ \frac{E_{Fo} - (E_2 - E_v)}{KT} \right\} \tag{2.34}$$

where E_{Fo} is the equilibrium Fermi level. For a PC activation energy of 0.2eV this model predicts an energy level for the E_2 states only 0.2eV below the Fermi level. In this model the mobility is assumed constant.

Regime 1 does not always involve a decreasing PC with increasing temperature (Wronski and Daniel, 1981). In regime 1 the lifetime is constant due to deep traps which keep p_R constant. They also assume that the mobility is constant.

The PC maximum occurs as regime 2, roughly defined by $n_{ph} > n_o$, is entered upon further decreases in temperature. A possible explanation for the maximum and the change in sign of the activation energy is due to the energy level of hole generation. In regime 2 the holes must reach recombination centres by moving from the valence band edge instead of the Fermi level, as in regime 1. This change in the initial level of the hole is expressed by (Simmons and Taylor, 1974)

$$J_{ph} = q\mu E \left\{ \frac{GN_o}{V\sigma_n N_t} \right\}^{1/2} \exp \left\{ \frac{(E_2 - E_v)}{kT} \right\} \qquad (2.35)$$

where the activation energy is now equal to E_2. An alternate approach is that as regime 2 is entered the hole quasi Fermi level moves closer to the recombination centres, E_2, below midgap. This causes holes to be fully available for recombination (Shirafuji et al, 1985). If the dominant recombination process is from E_1 to E_2, then

$$J_{ph} \sim (G)^{1/2} \exp \left\{ \frac{-(E_c - E_1)}{kT} \right\} \qquad (2.36)$$

However, if the transition from E_c to states near E_{Fo} limits recombination, we have

$$J_{ph} \sim G \exp \left\{ \frac{-(E_c - E_1)}{kT} \right\} \qquad (2.37)$$

We might also say that the lifetime of electrons becomes constant as J_{ph} enters regime 2 and so the decrease in PC and the PC maximum are caused by the activated mobility (Mott and Davis, 1979), with

$$J_{ph} \sim (\mu_D)^{-(1/2)}$$

Finally, the decrease of PC in regime 2 could be attributed to the gradual incorporation of states above the midgap into the recombination process (Wronski and Daniel, 1981). This causes the density of p_R states to increase with decreasing temperature and relates the activation energy to the depth of the trapping centres below the conduction band.

Clearly there is no concensus on the appropriate interpretation of these two regimes. Each of the models that have been reported are applicable in certain situations, but are not completely consistent. Specifically, we feel that it is necessary to account for the position of the equilibrium Fermi level when comparing films (Wronski and Daniel, 1981; Pickin, 1983).

As the temperature continues decreasing either regimes 3 and 4 will be observed, or regime 5 will be observed at low temperature. The low temperature PC maximum which separates regimes 3 and 4 is not always observed, but has been analyzed on the basis of a deep level of traps below the midgap (Rose, 1963; Vanier et al, 1981). The general characteristics of this maximum are: (1) a shift in the temperature of the maximum to higher values as the light intensity increases; and (2) a supralinear dependence of the PC on the photon flux on the high temperature slope. To explain this behaviour we can again use a two level approach (Rose, 1963) although three or more levels could also be used (Bube, 1960; Hoffman and Stockmann, 1979). We assume that some distribution of states 1 are below the midgap, with $\sigma_{n1} << \sigma_{n2}$, and states

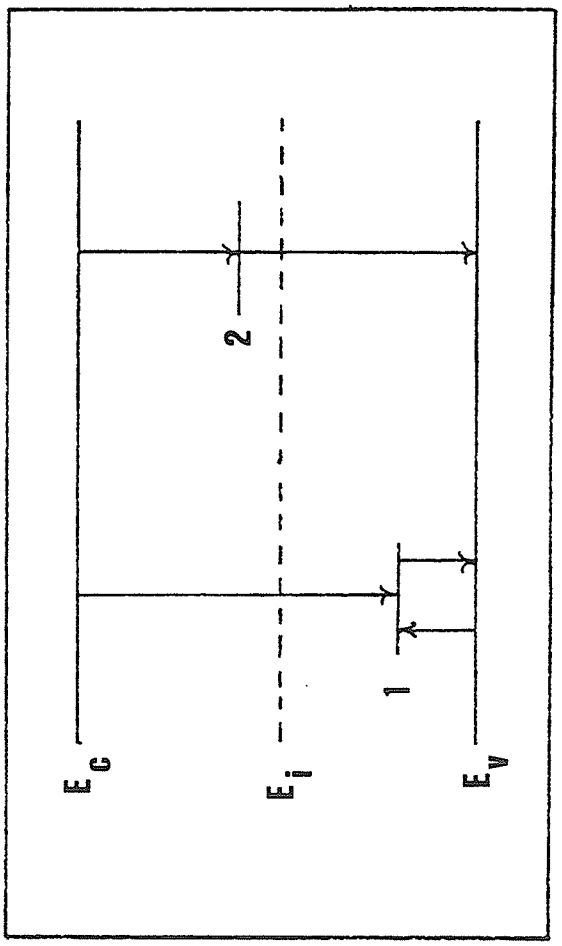

FIGURE 2.7. A two state model to explain the low temperature PC maximum and supralinearity in the PC intensity dependence. The class 1 and class 2 states are indicated.

2 are near the midgap. This model is shown in Figure 2.7. In regime 2 the quasi Fermi levels move toward the band edges as the temperature decreases. As the hole quasi Fermi level nears the class 1 states, it will change these states from hole traps to recombination centres. Because $\sigma_{n1} << \sigma_{n2}$, the class 1 states will fill with holes and thus the states 1 will dominate the recombination. The lifetime increases because $\sigma_{n1} << \sigma_{n2}$. As the temperature decreases further, the hole quasi Fermi level will convert all of the class 1 states into recombination centres, and thus the lifetime becomes constant. The PC maximum is caused by assuming an activated mobility. As the light intensity is changed, the temperature at which the PC maximum occurs will change as well. The amount of the temperature shift will indicate the energy level of the class 1 states.

The first interpretation of this phenomenon in a-Si:H films was made by Vanier et al (1981) although the presence of a bump or shoulder had been observed by other investigators (Kougiya et al, 1980; Anderson and Spear, 1977). The appearance of the maximum is dependent on an equilibrium Fermi level located near the midgap and on a low defect density (Vanier et al, 1981; Persans, 1982).

The low temperature regime in a-Si:H films, regime 5, generally is characterized by a constant value of the PC for a specific intensity of illumination. In this region the quasi Fermi levels are very near to the band edges for all of the light intensity levels which are used. We could

interpret regime 5 as being due to a constant lifetime (Simmons and Taylor, 1974) caused by the complete conversion of the gap states into recombination centres. This implies that the onset of the regime should be light intensity dependent and that the mobility and quantum efficiency are assumed constant.

An alternative explanation uses offsetting temperature dependences to obtain the constant photocurrent (Mott and Davis, 1979). If the carriers are trapped by deep neutral centres and recombine before any quasi-equilibrium is established, then

$$\frac{1}{\tau} = N v_{ph} \exp\left(\frac{-W}{KT}\right) A \qquad (2.39)$$

and if a hopping mobility is assumed, the mobility is

$$\mu = \left\{\frac{qN_{ph}}{kT}\right\} \exp\ (-2\alpha a)\ a^2 \exp\left\{\frac{-W}{kT}\right\} \qquad (2.40)$$

and so the photocurrent is independent of temperature due to the offsetting temperature dependences of the lifetime and mobility.

Another explanation of the PC behaviour in regime 5 is based on the assumption that the low temperature PC is entirely due to the thermalizing carriers. In this case the carriers are trapped immediately after reaching the mobility edge and cannot contribute to the photocurrent (Hoheisel et al, 1983). This theory leads to a linear dependence of PC on intensity.

We now present, briefly, a mechanism which we feel might be important at low temperatures. We have already discussed the size and temperature dependence of the capture of the capture cross-section. We know that an attractive center with r=50Å at 300°K will expand to r=500Å at 30°K. However, if the density of states in the gap is $10^{16}/cm^3$, these defect centers are only 350Å apart. Clearly, there must be significant overlap of these centres at low temperatures, which should cause the expression for the lifetime at high temperatures to be invalid. An analysis based on this mechanism has not yet been done.

Another possible mechanism which might be important is the temperature dependence of the capture cross-section in the range of temperatures from 300°K to 30°K. If the lifetime is dominated by a neutral or attractive center at high temperatures, it could become dominated by a repulsive center at low temperatures. This would occur because the repulsive centers have a much stronger temperature dependence than the neutral or attractive centres (Milnes, 1973).

The Effects of Light Intensity

The relationship between the photoconductivity and the light intensity is usually characterized by an equation of the form

$$J_{ph} \sim G^{B} \tag{2.41}$$

where

$$G = G'(1-R)\ (1-\exp(-\alpha d)\ \eta/d \tag{2.42}$$

Typically, the value of β ranges from 0.5 to 1.0, however, other values have been reported (Wronski and Daniel, 1981; Hack et al, 1984; Vanier et al, 1981). The value of β is dependent on light intensity and temperature and is normally analyzed in the following way (Rose, 1963). The only variable of the PC equation, which changes with the intensity is the lifetime. So far we have neglected the saturation effects, which would affect the absorption, and the possibility of intensity-dependent mobility effects. Because the capture cross-section is normally assumed to be independent of carrier density, at least to a first order approximation, and the microscopic velocity is dependent only on the temperature, the carrier lifetime should be dependent on the density of recombination centres, p_R. Specifically, if the value of β is less than 1, the density of recombination centres must be increasing as the intensity increases. If we now assume an exponential distribution of localized gap states, such that they may be expressed as

$$g(E) \sim \exp(-E/E_o) \tag{2.43}$$

where E_o is the characteristic energy. If we also assume that the quasi-Fermi level for electrons moves through this distribution as the light intensity increases, then the relationship between β and E_o may be written as (Evangelisti et al, 1983)

$$E_o = kT\beta/(1-\beta) \tag{2.44}$$

For instance, if β=0.75 at T=300 K, then E_o=0.08eV. However, there are two problems with Rose's interpretation of the value of β. First, it is clear from Equation 2.44 that the value of β should change in a prescribed manner, for a given value of E_o, as the temperature changes. This

behaviour is rarely observed. Secondly, the value of β should change rapidly as the quasi Fermi level moves through the gap because normally there are peaks and valleys in the gap state distribution (Evangelisti et al, 1983). These problems indicate that Rose's theory has a limited application for a-Si:H films.

There is, however, an alternative method of analysis which may prove useful for a-Si:H films. If we assume that recombination occurs as free electrons fall into recombination centres which have already trapped holes, and if these centres are positively charged when empty, then the steady-state photoconductivity and the charge neutrality equation may be written as (Evangelisti et al, 1983)

$$G - np_R v \sigma_n = 0 \tag{2.45}$$

$$n + \int_{E_{Fo}}^{E_c} n_t(E)dE = p_R \tag{2.46}$$

where G is given by Equation 2.42 and v_n and p_R denote the capture coefficient and the density of recombination centres, respectively. If the gap state distribution $N_T(E)$ is a slowly varying function of energy, then

$$\int_{E_{Fo}}^{E_c} n_t(E)dE = kT\bar{N}_T \text{ In } (n/no) \tag{2.47}$$

where $\bar{N}_T$ is the average density of localized states. Solving these equations yields

$$G - v\sigma_n (n^2 + n\bar{N}_T kT \text{ In}(n/no)) = 0 \tag{2.48}$$

This equation yields the desired range of β if $\bar{N}_T$ and G are chosen such that the second term inside the parenthesis is larger than the first. This equation is only applicable for the case $n>n_o$.

For values of β which are greater than 1 or less than 0.5 separate analysis techniques must be used. To explain the presence of supralinearity, $\beta>1$, we have already stated the appropriate model. The two-state model which was used to explain the low temperature PC maximum also explains the presence of supralinearity (Rose, 1963). Because $\sigma_{n1} << \sigma_{n2}$ the lifetime will increase quickly as the intensity and temperature pass through a certain range. Other explanations of supralinearity include a mobility which increases with increasing intensity or a capture cross-section which increases as the density of electrons increases (Persans, 1982; Bube, 1960). These explanations are not generally used.

To explain lower values of β, such that $\beta < 0.5$, we can use the concept of charge neutrality to develop a model (Hack et al, 1984). In this model it is assumed that there is a steeply rising distribution of states just above the quasi Fermi level, such that $E_o < kT$. This will cause a relatively large density of electrons to be trapped, and thus the positively charged recombination centre density will increase rapidly also, leading to $\beta < 0.5$. Another explanation could include two sets of gap states, both of which contribute to the recombination traffic. Any

movement of the hole and electron quasi Fermi levels could then contribute twice the amount of empty recombination states, and $\beta < 0.5$ could occur.

The Effect of Photon Energy

The response of the photoconductivity to changes in the photon energy is useful for understanding optical transitions (Moddel et al, 1980; Vanecek et al, 1981), geminate recombination (Adler et al, 1984; Moddel et al, 1981; Carasco and Spear, 1983) and the behaviour of the absorption coefficient for weakly absorbed photon energies (Loveland et al, 1974; Cody et al, 1980; Abeles et al, 1980; Moustakas, 1980; Vanecek et al, 1981; Moddel et al, 1980). As the photon energies decrease from $hv > E_g$ to $hv < E_g$ two important effects occur. First, the importance of surface effects, such as surface recombination and band-bending, decreases as the photon energy decreases. This occurs because a larger fraction of the absorption occurs in the bulk. Surface phenomena have not been well studied for a-Si:H films, and have been virtually excluded in this thesis. These effects, however, would become increasingly important as our understanding of the bulk properties of these films grows (Street et al, 1985). Secondly, the importance of geminate recombination and hopping transport may increase as the photon energy decreases (Carasco and Spear, 1983).

In the literature the effect of photon energy has not been thoroughly studied. Some investigators have reported that the value of B decreases towards 0.55 as the photon energy decreases to 1.0eV (Evangelisti et al, 1983). The photoconductivity as a function of temperature does not change for photon energies $h\nu > E_g$ (Adler et al, 1980), which is in keeping with a constant thermalization time for the photon energy range 2.3eV to 1.8eV (Vardeny and Tauc, 1981). There is also evidence from photoluminescence studies that sub-band gap photon energies will create non-radiative recombination centres, N_R, which may be expressed as (Bhat et al, 1983)

$$N_R \propto (G)^{1/2} \qquad (2.49)$$

This effect can be easily understood if we allow the initial state of the optical transition to be the same state which controls the recombination traffic. Therefore, for every electron which is photo-excited there will be a photo-excited hole also, and therefore we have essentially bimolecular recombination. The other effects that are observed could be explained by a change in the final state of the optical transition. However, this theory will require further work to verify its validity (Moddel et al, 1980; Persans, 1982).

The Effect of the Applied D.C. Field

Generally, the electric field is used as a tool for determining the importance of geminate recombination. As the field increases to values above a critical field (Adler et al, 1980) the geminate recombination

becomes negligible. This expected behaviour, based on Onsager's theory, has already been discussed. Other effects due to the applied fields include the interaction between space-charge limited currents and the photoconductivity, although this has not been studied for a-Si:H films (Rose, 1963). Usually the applied field (d.c.) dependence is not studied.

CHAPTER 3: MICROCRYSTALLINE TO AMORPHOUS TRANSITION IN SILICON FROM MICROWAVE PLASMAS

We have studied the effect of the plasma confining magnetic field on the Si:H thin film properties, and have found that the films change phase: we obtain microcrystalline films (μc-Si:H) at low fields and amorphous films (a-Si:H) at higher fields. The field at which the transition between these two phases occurs is approximately equal to the field at which electron cyclotron resonance (ECR) occurs. We observe two sizes of microcrystallites for these films, the larger size ($\sim$ 150Å) increases in volume fraction as the magnetic field decreases, whereas the smaller size ($\sim$20Å) maximizes its volume fraction at the ECR condition.

Interest in microcrystalline silicon (μc-Si) prepared by radio-frequency (RF) glow discharge and other deposition methods has recently arisen as a consequence of its superior electronic properties for specific applications as compared to amorphous silicon (a-Si:H) (Veprek and Maracek, 1968; Mishima et al, 1982; Spear et al, 1981; Hamasaki et al, 1980; Hirose, 1982; Tonaka and Matsuda, 1983; Matsuda, 1983; Le Comber et al, 1983; Osaka and Imura, 1984; Iqbal and Veprek, 1982; Mejia et al, 1983; Mejia et al, 1986). Veprek and Maracek (1968) prepared μc-Si by chemical transport in a hydrogen plasma as early as 1968. More recently, the properties of μc-Si fabricated in RF glow discharge (eg. Mishima et al, 1982) or by sputtering (Le Comber et al, 1983; Osaka and Imura, 1984) have been reported. It has been claimed that the formation of the

microcrystallites is dependent upon the employment of low deposition rates and high RF power densities (Mishima et al, 1982; Tonaka and Matsuda, 1983) which provide for a high density of reactive hydrogen in the plasma and maintain quasi-equilibrium conditions for the plasma-substrate reaction kinetics (Iqbal and Veprek, 1982).

In this study we have employed a novel microwave plasma system (Mejia et al, 1983, 1986) in place of the conventional RF plasma and observed the controlled deposition of μc-Si at relatively high deposition rates and low microwave power density. One of the features of this system is an externally applied dc magnetic field B along the longitudinal axis of the wave guide cavity (Mejia et al, 1983), we show that a transition from microcrystalline to amorphous silicon can be facilitated simply by increasing B, while maintaining other plasma conditions constant. All of the silicon films contain bonded hydrogen. It is to be noted that Spear et al (1981) observed earlier that microcrystalline growth was induced most easily at the highest accessible RF frequencies.

Another interesting feature of the microwave plasma system employed in this work is that, as B is increased, the plasma can be made to pass through the point of electron cyclotron resonance (ECR) (Mejia et al, 1986). This is the condition for which the cyclotron orbits of the electrons induced by a B field is resonant with the microwave frequency which activates the plasma. In the present work, the microwave frequency used is 2.45 GHz and the value of B to achieve ECR is 875 gauss. In

Figure 3.1 we shown the room-temperature dark conductivity σ_d, the average grain size of the microcrystallites in the (111) orientation δ, and the deposition rate r as functions of the normalized magnetic field (NMF, normalized to unity for B of 875 gauss - ECR condition). Our conclusion is that below ECR we obtain μc-Si:H; above ECR the films are amorphous.

Figure 3.2 shows typical x-ray diffraction results for Si:H films for various values of B; below and above ECR, as well as approximately at the ECR condition. In the analysis of the diffraction data for all of the film samples prepared, we have adopted the conventional approach (Klug and Alexander, 1954) of inferring the average crystallite size (as employed in Figure 3.1) from the full-width-at-half maximum of the (111) diffraction peak using Scherrer's formula (Mishima et al, 1982) and a shape factor equal to 0.89. We have also made x-ray diffraction measurements of the (220) and (311) peaks and have found a large scatter in the values of the cube edges. Because of this scatter we could not determine the general shape of the crystallites.

By comparing our data with those of other investigators (Mishima et al, 1982; Tonaka and Matsuda, 1983) we note that the thermally crystallized films have a ratio of the peak intensity to the background intensity of $\sim$3-4 and that our films deposited at NMF = 0.55 have the same ratio. From this data we estimate an upper bound on the microcrystallite volume fraction to be 100%; and by comparing the dc conductivity with RF glow discharge produced microcrystalline film we

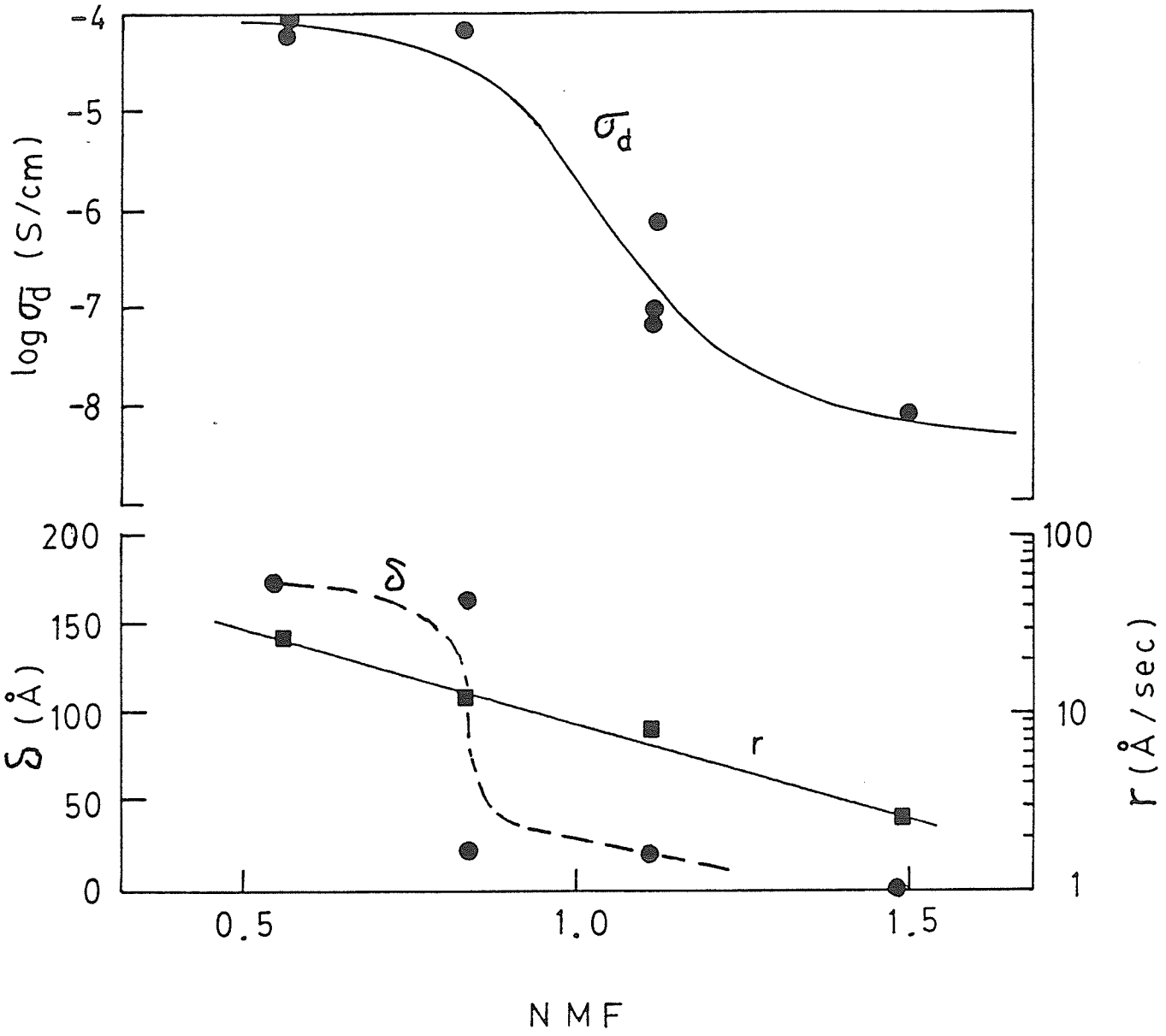

FIGURE 3.1. The room temperature dark conductivity σ_d, the average grain size of the microcrystallites in the (111) orientation δ, and the depositin rate r, as functions of normalized magnetic field(NMF).

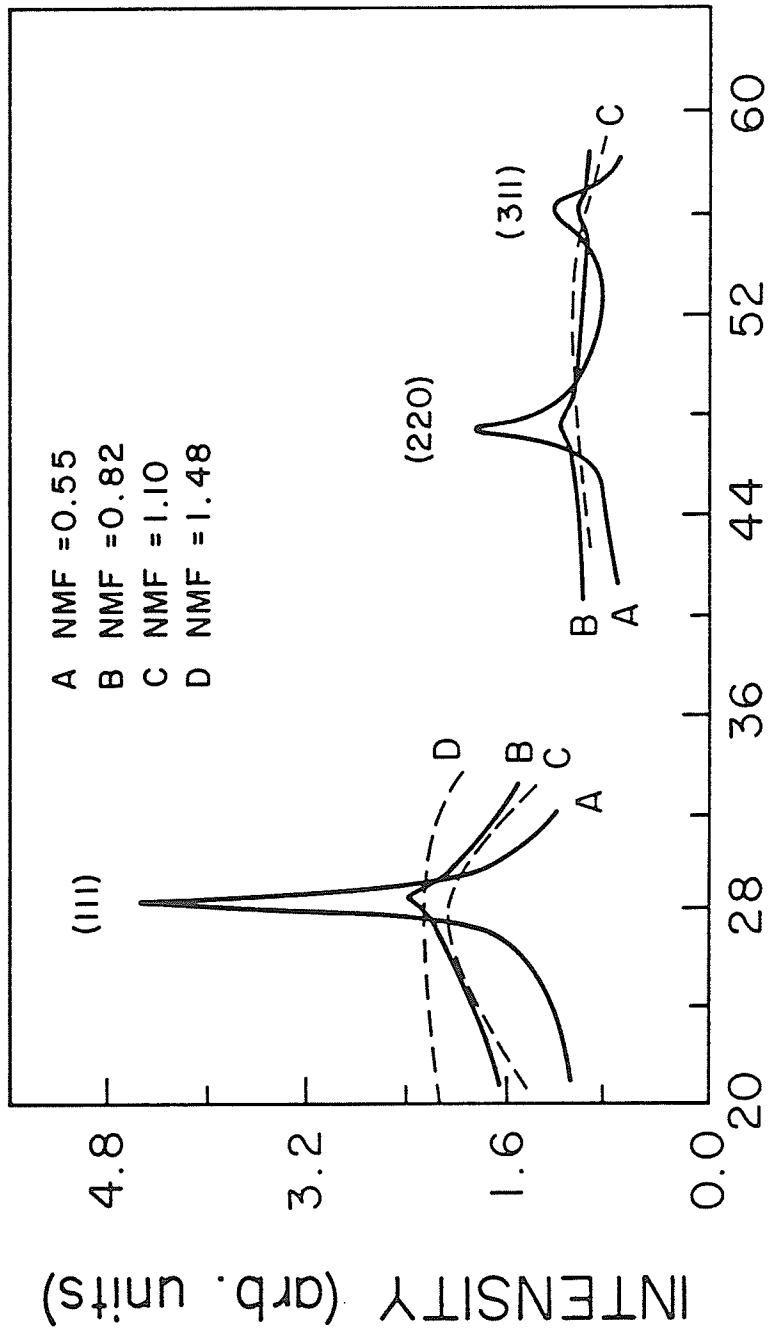

FIGURE 3.2. Typical X-ray diffra tion results for Si:H films.

estimate the lower bound on the microcrystallite volume fraction to be 50%. As B is increased the films become a three-phase material, being a mixture of a-Si:H, 20A μc-Si:H, and 150A μc-Si:H. We also note that the 20A μc-Si:H phase has peak diffraction amplitudes at $2\theta = \sim 27.5^{\circ}$ and 51.0°, which are significant shifts from the peak positions of the 150Å μc-Si:H phase. This implies that there may be internal pressure on the 20A microcrystallites (Cullity, 1956).

The deposition rate r for all the samples under investigation was in the range of 4 to 24 A/sec. The deposition rate was dependent upon the position and orientation of the substrates in the wave guide cavity, as described elsewhere (Mejia et al, 1983). The microwave power in Figure 3.1 was in the range of 1 to 7 watts and the (glass) substrate temperature was 155C.

We have also performed extensive studies of both the plasma characteristics and the electronic properties of the deposited Si:H thin films. The microwave system appears to have several decided advantages over RF systems in addition to the flexibility as reported here. The electronic properties of the μc-Si:H and a-Si:H films, including dark conductivity and photoconductivity, are essentially the same as those prepared by RF glow discharges (Mishima et al, 1982; Matsuda, 1983). More details on plasma characteristics and film properties will be reported later.

As explained by Matsuda (1983) among others, the customary dilution of SiH_4 in H_2 or other gases is not a prerequisite for uc-Si:H structures. Instead, he draws attention to the ratio of the concentration of atomic hydrogen H in the plasma to the film deposition rate. The H concentration is determined by optical emission spectroscopy (OES) from the intensity of the H_2 line at 656.3nm (Mirose, 1982; Matsuda, 1983). The proportionality between r and the SiH emission at 412.7 nm reported by Matsuda (1983) was not observed for our microwave plasma conditions. The IR absorption peak associated with SiH bonds in our films is consistent with the RF data (Mishima et al, 1982). However we have relatively less SiH_2 bonding present with the microwave films.

While the optical gap does not change significantly, the activation energy decreases, and thus the Fermi level increases, appreciably in the transition from amorphous to microcrystalline structure, as shown in Figure 3.3. This implies that the increase in the degree of microcrystallinity tends to enhance the n-type behaviour of the Si:H films. It is also interesting to note that the photoconductivity exhibits a minimum value at the point where the dark conductivity is around 5×10^{-7} S/cm, which corresponds to the film deposition condition close to ECR as shown in Figure 3.4. This phenomenon is similar to that observed by Mishima et al (1982) for their films prepared in a RF plasma.

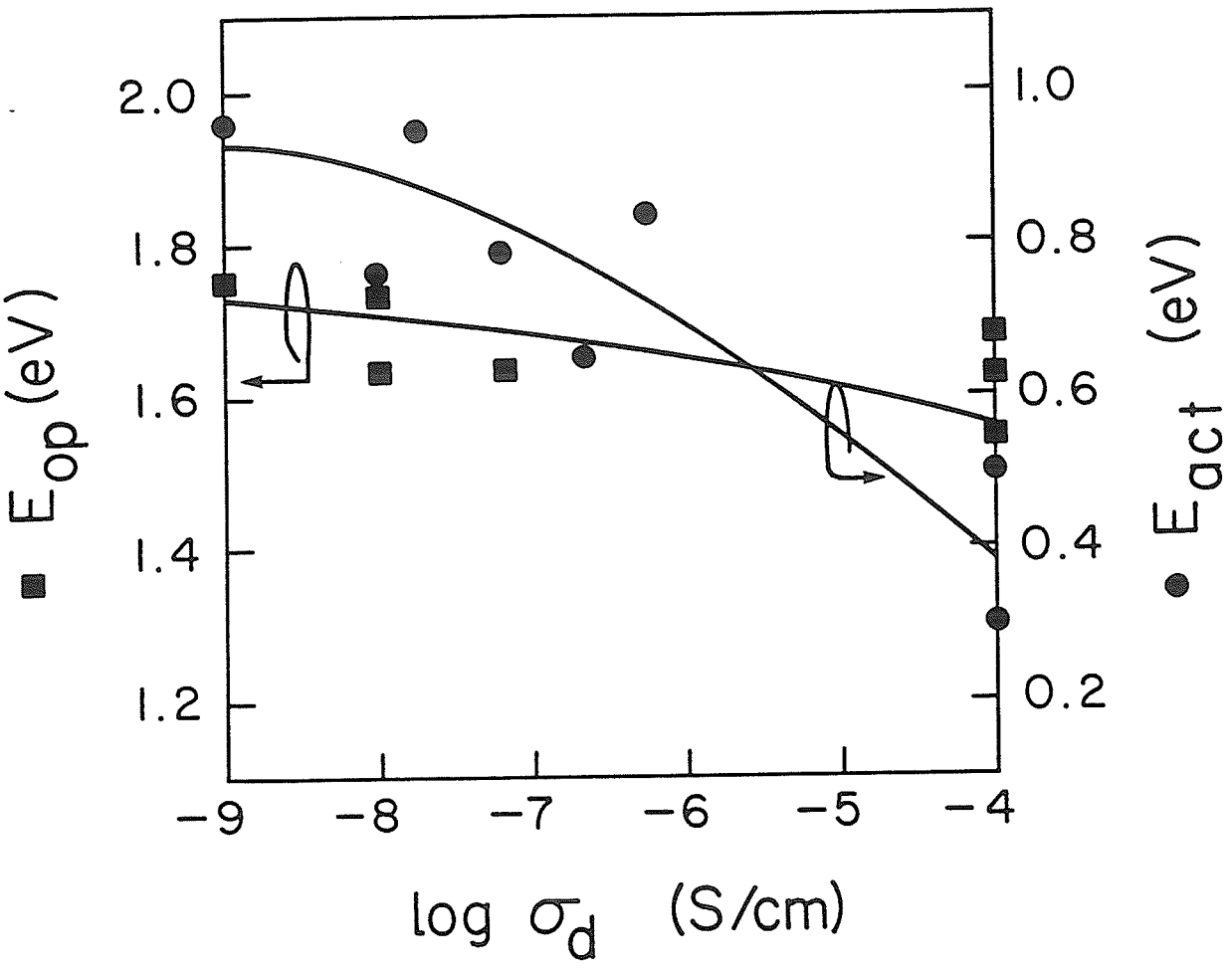

FIGURE 3.3. The optical gap and the activation energy against the dark conductivity.

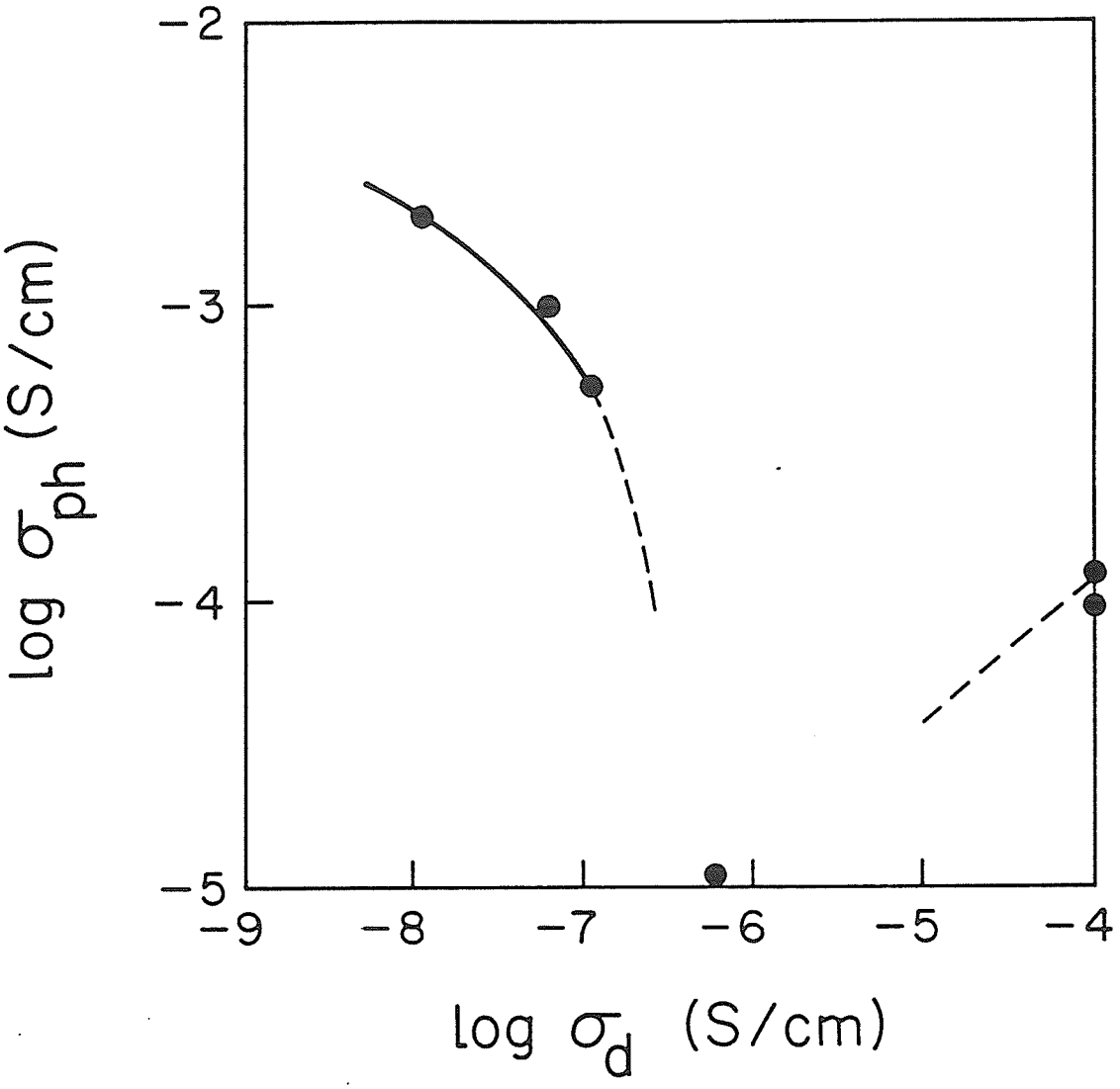

FIGURE 3.4. Room temperature photoconductivity against the dark conductivity.

In summary, the condition of ECR in microwave plasmas has been found to provide a demarcation between μc-Si and a-Si:H formation. The microwave plasma system is also observed to provide several advantages over RF plasmas, including reduced power requirements and enhanced deposition rates for both μc-Si and a-Si:H films. The film properties are comparable to the best RF glow discharge films.

CHAPTER 4: PHOTOCONDUCTIVITY OF a-Si:H FILMS

In this chapter we report on the effects of temperature, light intensity and phonton energy on the photoconductivity. We discuss these observations in terms of the relative density, distribution, and capture parameters of the localized gap states and the temperature dependence of the capture parameters. We have calculated the distribution of states both above and below the midgap, and developed a new theory to explain the relationship between photoconductivity and light intensity. The measurement of the spectral response of the photoconductivity is used to obtain the information on the density and distribution of states below the midgap. Finally, we present a new interpretation of the low temperature photoconductivity (PC) maximum, which gives evidence that there is a maximum and minimum in the density of states above the midgap. The experimental methods and the deposition conditions for each experiment and sample are given in the Appendix.

4.1 The Absorption Coefficient of a-Si:H Films for Sub Band Gap Photon Energies

We have found that as the equilibrium Fermi level decreases from 1.2eV to 0.89eV above E_v the form of the absorption spectra changes significantly. At hv=1.3eV there is a peak in the absorption for the sample with the lowest value of E_{Fo}. This behaviour may be associated with an increasing density of states at 1.3eV below E_c. Also, we have found that for lower photon energies, $hv \leq 1.2$eV, there are transitions from E_v into the localized states, which affects the photoconductivity (PC) through the reduction in the quantum efficiency. The value of the Urbach edge is $\sim$0.080eV to 0.060eV for these films.

Several methods have been proposed to extract the absorption spectra from the PC spectral response (Moddel, et al, 1981; Vanacek, et al, 1981; Evangelisti, et al, 1983). In this study we use the following two methods. First, if β, the parameter which is used to characterize the relationship between the photoconductivity and light intensity, is constant with photon energy, then the absorption coefficient, α, can be written as (Moddel, et al, 1981)

$$\frac{\alpha(hv)}{\alpha_o} = \frac{G_0}{G}\left\{\frac{J_{ph}(hv,G)}{J_{ph0}}\right\}^{1/\beta} \qquad (4.1)$$

where the subscript $_o$ refers to some reference energy, and G refer to the light intensity. Second, if β is dependent on the photon energy then the absorption coefficient can be written as (Evangelisti et al, 1983)

$$\alpha(hv+\Delta) = \alpha(hv)\frac{G(hv)}{G(hv+\Delta)}\left\{\frac{\Delta\sigma(hv+\Delta)}{\Delta\sigma(hv)}\right\}^{1/\beta(hv)} \qquad (4.2)$$

where Δ is the step size of the iteration and $\Delta\sigma$ refers to the photoconductivity. In both of these methods the light intensity is allowed to vary with the photon energy; but the mobility and quantum efficiency are assumed to remain constant as the photon energy is changed.

To study the relative values of the mobility and quantum efficiency we use the temperature dependence of the PC spectral response, as illustrated in Figure 4.1. The slope of the high energy part of the curve, for hv>1.45eV, does not change as the temperature decreases. As well, the form of the curve for hv<1.2eV becomes steeper at lower temperatures.

Figure 4.2 shows the activation energy of the PC as a function of photon energy. For hv<1.2eV the activation energy rises rapidly, indicating that the quantum efficiency or mobility is decreasing in this range of energies (Carasco and Spear, 1983). The dotted line in the figure indicates the fit to Onsager's relation, which implies that the quantum efficiency is causing the majority of this decrese in the PC. For these values of the activation energy we have calculated the value of r_0, the thermalization distance, and found that r_0 decreases from 100Å at hv=1.3eV to 20Å at hv=1.0ev. The response of the photoconductivity to the temperature also indicates that the mobility is not changing for hv>1.2eV (Moddel et al, 1981). Therefore, the absorption coefficient may be deduced from the PC spectral response.

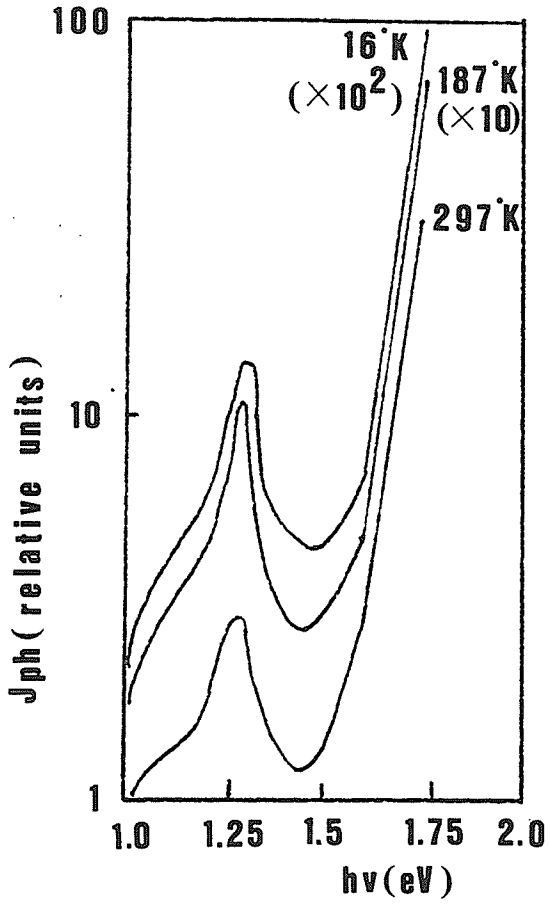

FIGURE 4.1. The PC spectral response as a function of temperature.

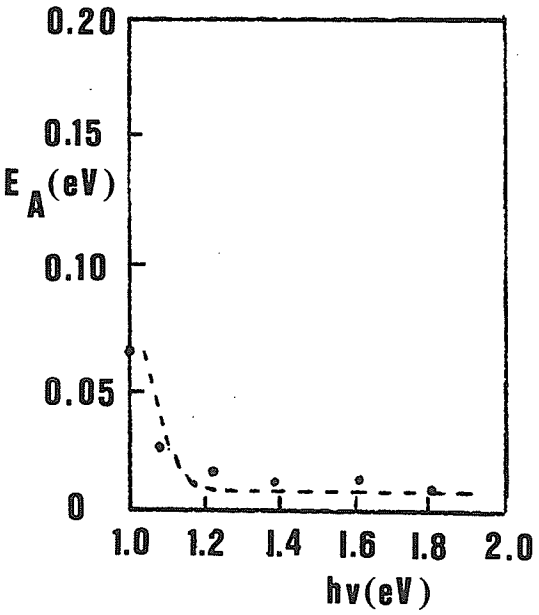

FIGURE 4.2. The activation energy as a function of photon energy. The dotted line indicates the fitting of Onsager's relation.

In Figure 4.3 we present PC spectral response for each of the four samples. There is an increase in the PC at hv=1.3eV, and a smaller increase at hv=1.1eV. In the same figure we also show the value of β for these samples. Sample 13V exhibits a value of $\beta<0.5$, but still in a consistent and repeatable manner. Generally, this low value indicates a rapid increase in the density of recombination centres (Rose, 1963), and not saturation. Therefore the absorption coefficients calculated from Equations (4.1) and (4.2) will still be accurate. Also, these low values of β indicate that the initial state of the electron transitions are increasingly occurring in the localized states as the photon energy decreases.

Figure 4.4 shows the absorption spectra calculated using Moddel's method by choosing $\beta=0.70$ as an average value. The absorption at hv=1.3eV changes form as the equilibrium Fermi level decreases from E_c , and peaks are visible for two of the samples. An extrapolation of two of the curves, as shown, indicates that the absorption goes to zero as the photoenergy goes to $E_c - E_{Fo}$. Of course, for $hv<E_c-E_{Fo}$, we expect no absorption unless there are transitions into localized states below E_c. This behaviour may be explained in two ways. First, it is possible that the fraction of the absorption caused by transitions into the localized states is larger for samples which have no peak at 1.3eV, and therefore these absorption curves do not cut off at the Fermi level. Secondly, we could assume that there is a constant density of states in the energy range 1.2eV to 1.4eV below E_c , and thus the density of states would abruptly decrease as $hv=E_c-E_{Fo}$ is reached.

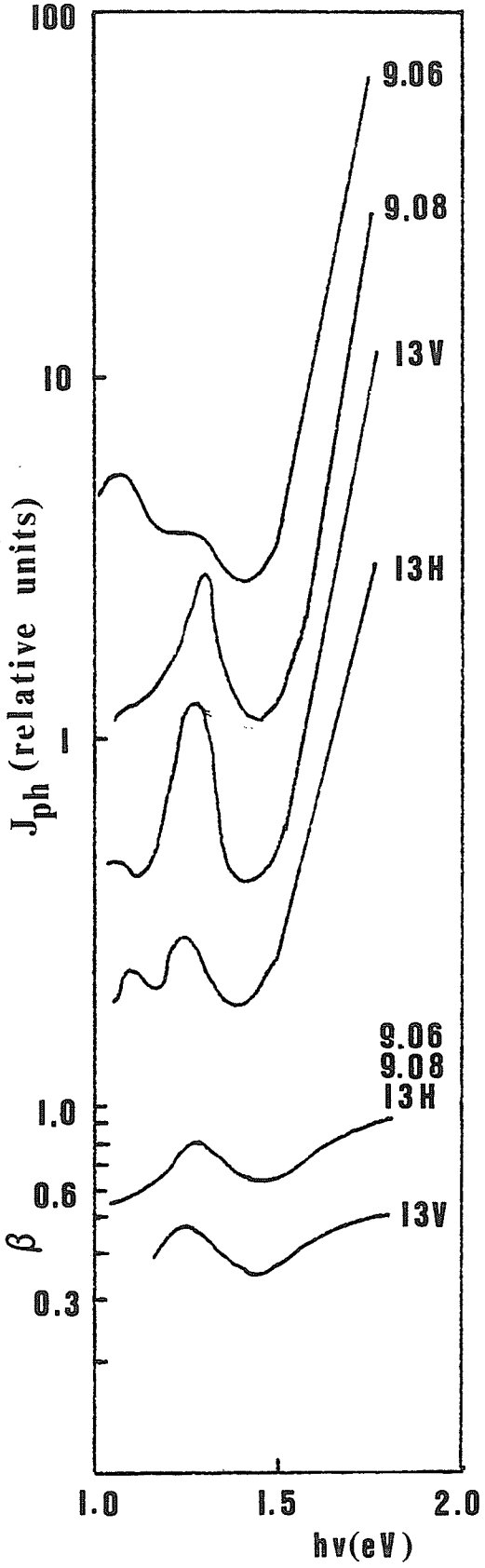

FIGURE 4.3. The PC spectral response and the value of β for $1.75eV \geq hv \geq 1.1eV$.

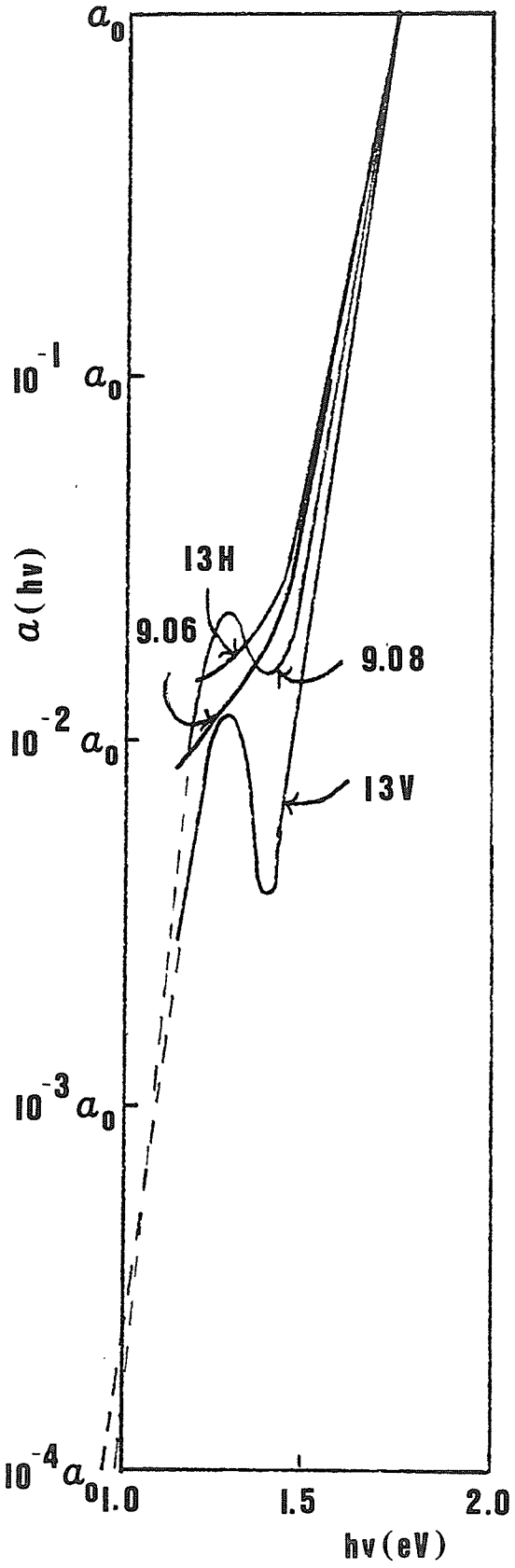

FIGURE 4.4. The absorption spectra as calculated by the constant β method (Moddel et al, 1980)

In Figure 4.5 we present the absorption spectra calculated using the iterative method (Evangelisti et al, 1983). The peak at hv=1.3eV is still large in sample 13V. However, the peak has decreased in sample 9.08 relative to those shown in the Figure 4.4. Samples 9.06 and 13H demonstrate the same behaviour as those calculated by the constant B method. The values of the Urbach edge slope, E_o, also vary between these samples, from $0.08eV>E_o>0.06eV$. Generally, these figures indicate that as the Fermi level decreases from E_c the value of E_o decreases and the peak at 1.3eV becomes more pronounced. These findings are in good agreement with other investigators (Loveland et al, 1974) who have reported that the relative absorption at 1.3eV increased as the Fermi level decreased towards midgap. Other investigators have also found that the peak at 1.3eV decreases with increasing hydrogen incorporation (Abeles et al, 1980) and that the Urbach edge slope, E_o, decreases as the temperature decreases (Tiedje and Cebulka, 1983).

These absorption spectra also lead us to speculate on the form of the gap states distribution below E_{Fo}. If the transitions for hv>1.2eV are into the same final state, then the density of states is proportional to the absorption coefficient (Vanacek et al, 1981). This would indicate that the form of the gap state distribution changes significantly as the Fermi level shifts. Alternatively, if the fraction of the transitions into localized states increases as the Fermi level increases towards E_c, then the density of states in the gap could increase. These changes in the gap state density should be apparent in both the room temperature

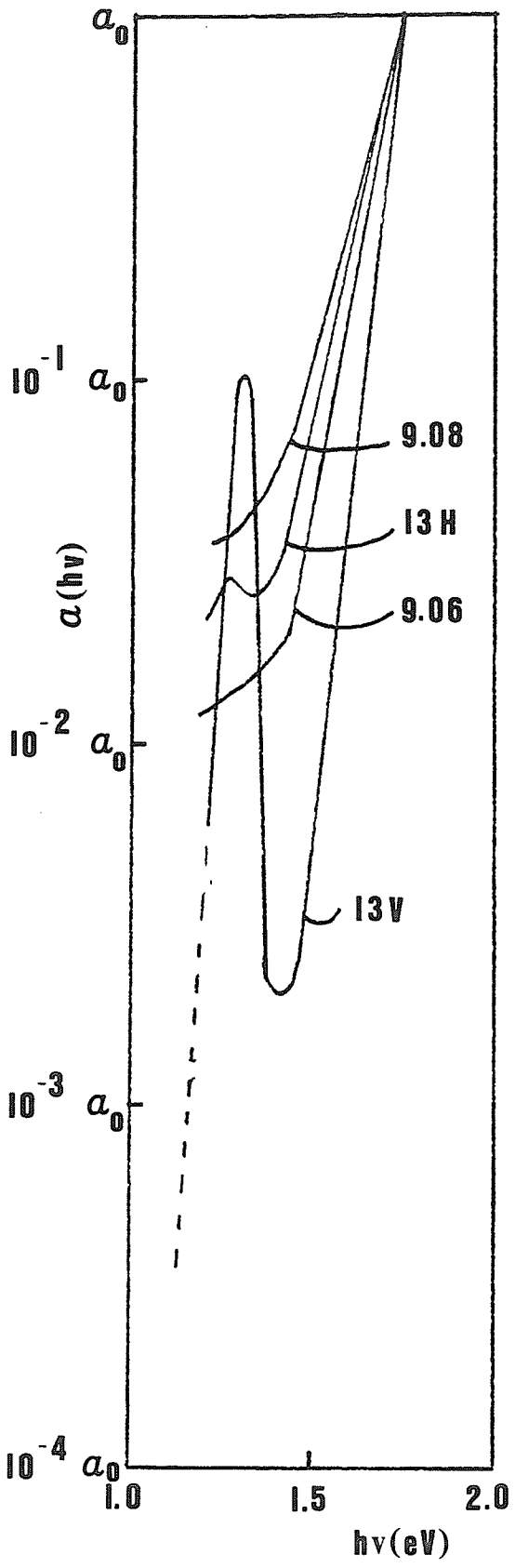

FIGURE 4.5 The absorption spectra as calculated by the iterative method(Evangelisti, et al, 1983)

electron lifetime and the response of the PC to light intensity. Further evidence of a sharp increase in the density of states below E_{Fo} is that $B<0.5$ is observed for sample 13V.

In conclusion, we have shown that the absorption coefficients of these films can be correlated with the position of the Fermi level. Specifically, as the equilibrium Fermi level decreases the absorption at hv=1.3eV changes shape and the slope of the Urbach edge decreases. The structure of the absorption curves can either be caused by a large density of states at 1.3eV below E_c, or an overall increase in the density of gap states, both above and below E_{Fo}.

4.2 The Intensity Dependence of the Photoconductivity in a-Si:H Films

In the following we present a new analysis of the light intensity dependence of the photoconductivity. This analysis considers the movement of both the electron and hole quasi Fermi levels and uses the charge neutrality condition to explain the value of β in a consistent manner. By assuming that the trapped charge dominates the charge neutrality equation, we can reproduce an earlier result by Rose (1963), and show that a similar type of equation can be used to explain other values of β, such as $\beta<0.5$ and $\beta>1.0$. We then obtain the density of states distribution for our films based on the observed relationship between the photoconductivity and the light intensity.

The relationship between the photoconductivity (PC) and the light intensity is generally characterized by an equation of the form (Rose, 1963)

$$\sigma_{ph} \sim G^{\beta} \tag{4.3}$$

where G is the light intensity and β is a parameter which is usually in the range of $0.5 \leq B \leq 1.0$.

Two theories of this behaviour have previously been proposed. The first theory is based on the assumption that the localized gap states above the Fermi level, g(E), are exponentially distributed in the gap, in the form

$$g(E) = A \exp\left\{\frac{-(E_c - E)}{kT_1}\right\} \tag{4.4}$$

and that the density of recombination centres, p_R , is negligible (in the dark) then the photogenerated electron density can be (Rose, 1963)

$$n = \left\{\frac{GN_c{}^{T/T_1}}{kT_1 Av\sigma n}\right\}^{T_1/(T_1 + T)} \tag{4.5}$$

where T_1 is the characteristic temperature of the distribution, A is the density of states at E_c and $v\sigma_n$ is the capture coefficients. The relationship between β and T can be expressed in terms of the characteristic energy of distribution, E_o, (Evangelisti et al, 1983)

$$E_o = kT\beta/(1-\beta) \tag{4.6}$$

The second theory is based on the assumption that the charge neutrality condition can be expressed as (Evangelisti et al, 1983)

$$n + n_t = p_t \tag{4.7}$$

where n and n_t are the densities of free and trapped electrons, respectively, and p_t is the density of trapped holes. Obviously, this assumption implies two types of defect states existing in the gap, one being negatively charged when filled and the other being positively charged when empty. The value of β can be deduced from

$$G - v\sigma_n(n^2 + n\bar{N}_T\, kT\, \ln(n/n_o)) = 0 \tag{4.8}$$

where n and n_o are the densities of photogenerated and thermally generated free electrons, respectively, and $\bar{N}_t$ is the average density of localized states at the Fermi level.

We have observed several problems with these two theories. First, Rose neglected any contribution to the density of recombination centres from the states below midgap. These states can affect the PC temperature dependence (Vanier et al, 1981; Wronski and Daniel, 1981), and so they must also affect the light intensity dependence. Secondly, neither one of these theories is able to account for power values of $\beta<0.5$, although these values appear as part of a steady trend with temperature and Fermi level position (Wronski and Daniel, 1981; Hack et al, 1984). Finally, calculations based on Rose's theory are not sensitive to a minimum in the density of states, although other techniques indicate that minima do exist (Goodman and Fritzsche, 1980).

In the following we present a new theory for the value of β, from which we can also calculate the energy distribution of the gap states above midgap and the relative form of the state distribution below midgap. We show that the distribution of states below the Fermi level also play a role in determining the value of β.

4.2.1 Theory

To develop a theory for the PC intensity dependence, we need to consider the following factors. First, in the steady-state, the generation rate (G) is equal to the recombination rate. If we assume ballistic capture of the free electrons (n) to be dominant recombination process, we have

$$G - v\sigma_n n p_R = 0 \tag{4.9}$$

where p_R is the density of recombination centres. For any two light intensities, G_1 and G_2 with $G_2 > G_1$, we have

$$\Delta G = \frac{G_2}{G_1} = \frac{n_2 p_{R2}}{n_1 p_{R1}} = \Delta n \Delta p_R \tag{4.10}$$

this equation applies for any change in light intensity as long as the value of $v\sigma_n$ remains constant.

Secondly, we need to consider the charge neutrality condition. If we neglect the charge due to free carriers, we obtain

$$n_t + n_R = p_t + p_R \tag{4.11}$$

where n_t and p_t are the trapped electron (hole) densities and n_R and p_R are the densities of filled and empty recombination centres located above and below the midgap, respectively. If

$$n_R = p_R \tag{4.12}$$

then we can express the charge neutrality as

$$\Delta n_R = \frac{n_{R2}}{n_{R1}} = \Delta p_R = \frac{p_{R2}}{p_{R1}} \tag{4.13}$$

Similarly, if the charge neutrality equation is

$$n_t = p_t \tag{4.14}$$

then

$$\Delta n_t = \Delta p_t \tag{4.15}$$

where $\Delta n_t = n_{t2/nt1}$ and $\Delta p_t = p_{t2/p_{t1}}$. The trapped charge is determined from the Fermi level position, whereas the charge in the recombination centres is determined according to the recombination kinetics. There are two mechanisms that can cause the density of recombination centres, either n_r or p_R, to change: (1) the traps can be converted into recombination centres by the movement of the Fermi level, and (ii) the ratio of the density of free electrons to that of free holes can change, due to unequal movements of the quasi Fermi levels. These two possibilities are shown by the following equation.

$$\Delta p_R = \Delta N_R \Delta p \left(\frac{\sigma_n n_1 + \sigma_p p_1}{\sigma_n n_2 + \sigma_p p_1}\right) \tag{4.16}$$

where $\Delta N_R = N_{R2/N_{R1}}$ is the increase of the recombination centres due to the conversion of traps, n and p refer to the free electron and hole densities, and the subscripts 1 and 2 refer to the light intensities G_1 and G_2, rspectively. Of course, Δp is still equal to p_{2/p_1}, the ratio of free holes at two light intensities.

We express the distribution of gap states as,

$$g_1(E) \sim \exp(-E/E_1) \qquad (4.17)$$

$$g_2(E) \sim \exp(-(E_c - E)/E_2)$$

where $g_1(E)$ refers to the density of states below midgap and $g_2(E)$ refers to the density of states above midgap, and E_1 and E_2 are the characteristic energies of the two distributions. Thus, for a change in the quasi Fermi levels of $\Delta E_{fn} = E_{fn2/E_{fn1}}$ (or $\Delta E_{fp} = E_{fp2/E_{fp1}}$), the change in the free and trapped charge densities is

$$\Delta n = \exp(\Delta E_{fn/kT}) \qquad (a)$$

$$\Delta p = \exp(\Delta E_{fp/kT}) \qquad (b) \qquad (4.18)$$

$$\Delta n = \exp(\Delta E_{fn/E_2}) \qquad (c)$$

$$\Delta p = \exp(\Delta E_{fp/E_1}) \qquad (d)$$

Similarly, we can express the change in the density of recombination centres as

$$\Delta p_{R1} = \exp(\Delta E_{fp/E_1}) \qquad (a)$$

$$\Delta n_{R2} = \exp(\Delta E_{fn/E_2}) \qquad (b) \qquad (4.19)$$

if we assume that (1) the density of recombination centres at E_{Fo} is much smaller than the density of centres at E_{fn}, or E_{fp}, and (2) if we neglect any change in the ratio $n/_p$ that would affect the density of these recombination centres.

Based on equations (4.18) and (4.19) we shall calculate β for several different conditions, and then go on to analyze the results from our a-Si:H films. We begin by specifying how the value Δp_R is controlled by charge neutrality conditions, and then show the value of β which results.

CASE 1: If we assume that the charge neutrality equation is

$$\Delta n_t = \Delta p_t \tag{4.20}$$

which means that the trapped charge dominates the total charge neutrality condition then we can write

$$\exp(\Delta E_{fn/E_2}) = \exp(\Delta E_{fp/E_2}) \tag{4.21}$$

and therefore,

$$\Delta E_{fp} = (E_1/E_2)\Delta E_{fn} \tag{4.22}$$

We now have the following four possibilities.

(a) If recombination proceeds mainly through the trapped holes, Δp_t, then by Equation (4.10)

$$\Delta G = \frac{G_2}{G_1} = \exp(\Delta E_{fn/kT})\exp(\Delta E_{fp/E_1}) = \exp(\Delta E_{fn/kT} + \Delta E_{fn/E_1}) \tag{4.23}$$

Generally a factor of $\exp(\Delta E_{fp/kT})$ is used to adjust the density of holes to compensate for its increased contribution to the recombination traffic (Rose, 1963). This factor is not applicable in this case because we have not changed the value of $E_{fp}-E$, but have instead only increased the density of the recombination centres. Since

$$\Delta E_{fn} = kT \ln(\Delta n) \tag{4.24}$$

we have

$$E_2 = kt\beta/(1-\beta) \tag{4.25}$$

where we have used $\beta = \ln(\Delta n)/\ln(\Delta G)$. This result is the same as that obtained by Rose (1963). If $E_2 < kT$ then $\beta < 0.5$, and if $E_2 \geq kT$ then $\beta \geq 0.5$. It is clear that the slope of the distribution of the states above midgap is very important for the determination of the value of β.

(b) If recombination occurs through the P_R states above E_{fp} and below E_{Fo}, we cannot express this change in recombination centre density by directly applying a Fermi level analysis. We must express the fraction of $g_1(E)$ states which are empty recombination centres as (Rose, 1963)

$$P_R = \frac{N_{R1}\ (\sigma_p p)}{(\sigma_p p + \sigma_n n)} = N_{R1}\alpha_1 \tag{4.26}$$

where

$$N_{R1} = \int_{E_{fp}}^{E_{Fo}} g_1(E)\ dE \tag{4.27}$$

The value of α_1 is in the range $0 \leq \alpha_1 \leq 1$, and is not expected to change as the level E_{fp} moves, and so any change in P_{R1} is totally due to an increase in the density of states between E_{fp} and E_{fo}. Therefore, for a movement of the Fermi level, ΔE_{fp}, we will change the value of N_{R1} by the factor

$$\Delta N_R = \exp(\Delta E_{fp/E_1}) \tag{4.28}$$

However, only a fraction α_1 will be empty and will contribute to recombination, therefore

$$\Delta p_{R1} = \exp(\Delta E_{fp/E_1}) \alpha 1 \tag{4.29}$$

Thus, the value of β can be determined from

$$\Delta G = \alpha_1 \exp(\Delta E_{fn/kT} + \Delta E_{fn/E_2}) \tag{4.30}$$

where we have used $\Delta E_{fp/E_1} = \Delta E_{fn/E_2}$. If we assume that $\alpha 1 = 1$, that is, that all incorporated centres are empty, then

$$E_2 = kT\beta/(1-\beta) \tag{4.31}$$

which is again equivalent to the equation derived by Rose (1963). If α_1 decreases from unity, the density of recombination centres does not increase as rapidly, and thus β approaches unity.

(c) If recombination occurs through the empty states below E_{fn} ($p_{R2} = N_{R2} - n_{R2}$), then the same type of analysis can be used as in the previous case (b). If p_R is negligible in the dark, and $\alpha_2 = 1$, then the value of E_2 is again

$$E_2 = kt\beta/1-\beta) \tag{4.32}$$

If $\alpha_2 < 1$, the value of β increases towards unity.

If $\alpha_2 < 1$, the value of β increases towards unity.

(d) If the recombination occurs through the empty states above E_{fn}, then the density of empty states increases as

$$\Delta p_t = \exp(\Delta E_{fn/E_2}) \tag{4.33}$$

Therefore, the value of β is determined from

$$\Delta G = \Delta n \Delta p_R = \exp(\Delta E_{fn/kT} + \Delta E_{fn/E_2}) \tag{4.34}$$

which means that

$$E_2 = kt\beta/(1-\beta) \tag{4.35}$$

As in case (a), the factor $\exp(\Delta E_{fn/kT})$ is not included.

(e) We now assume that the density of states above midgap decreases with increasing energy ($E_2 < 0$), which would occur if there is a local maximum in the density of states at some energy between E_{Fo} and E_c. In this case the change in the density of trapped charge is less than unity. The charge neutrality condition is still expressed as

$$\Delta n_t = \Delta p_t \tag{4.36}$$

and so the following possible results apply.

(i) For recombination through the Δp_t states below E_{fp}, we have a decrease in the trapped hole charge, and so

$$\Delta G = \Delta n \Delta p_t = \exp(\Delta E_{fn/kT} - \Delta E_{fn/E_2}) \tag{4.37}$$

This leads to

$$E_2 = kT\beta/(\beta-1) \tag{4.38}$$

Therefore, this means that $\beta>1$. We must interpret this value of $E_1 (E_1<0)$ as indicating that the level E_{fp} also goes through a decreasing density of states.

(ii) If recombination proceeds through the p_R states between E_{fp} and E_{fo}, we have $\Delta p_R = 1$, and $\beta \sim 1$. This is because the density of states decreases, and thus very little new states are added.

(iii) If recombination is through the empty states between E_{fo} and E_{fn}, then we expect a constant density of recombination centres, and thus $\beta = 1$.

(iv) If recombination occurs mainly through the empty states above E_{fn}, then we have

$$\Delta p_{t2} = \exp(-\Delta E_{fn/E_2}) \tag{4.39}$$

of course, $E_2<0$, and so $\Delta p_{t2}<1$. We then have

$$\Delta G = \Delta n \Delta p_{t2} = \exp(\Delta E_{fn/kT} - \Delta E_{fn/E_2}) \tag{4.40}$$

which gives

$$E_2 = kT\beta/(\beta-1) \tag{4.41}$$

This condition states that the density of trapped holes decreases as the E_{fn} level increases towards E_c, and so $\beta>1$ may be realized.

We observe that if the recombination is dominated by transitions through the trapped charge then $\beta>1$ can be realized. For a density of states in which the distribution is throughout the gap, we do not expect

that trapped charge will dominate the behaviour. We now continue to analyze other possible forms of the charge neutrality equation.

CASE 2: If we assume that the charge neutrality equation is

$$\Delta n_R = \Delta p_R \tag{4.42}$$

then, for exponentially increasing gap state distributions, we have the same relationship as before

$$\Delta E_{fp} = \frac{E_1}{E_2} \Delta E_{fn} \tag{4.43}$$

Therefore, all the previous cases (1a) to e)iv) apply.

Case 3: If we now assume that the charge neutrality equation is

$$p_{R1} = n_{R2} + n_{t2} \tag{4.44}$$

then we find that this equation cannot be expressed in terms of the changes in the densities of the trapped electrons and the recombination centres. We will, however, analyze this equation for the specific situation of $E_2<0$.

For this case, we know that the density of trapped charge is decreasing. If we assume that the density of positively charged centres is still increasing, then n_R will need to compensate both the decrease in n_t and the increase in p_R.

(a) If recombination is through p_t, then we have

$$\Delta p_t = \exp (\Delta E_{fp/E_1}) \tag{4.45}$$

and therefore, β can be deduced from

$$\Delta G = \Delta n \Delta p_t = \exp\left\{\frac{\Delta E_{fn}}{kT} + \frac{\Delta E_{fp}}{E_1}\right\} \qquad (4.46)$$

There is no simple relationship between ΔE_{fn} and ΔE_{fp}, and so we are content to state the $\beta<1$ because both p_t and n are increasing.

(b) For recombination through p_R, the same analysis applies as in subcase (a). Therefore we expect that $\beta<1$.

(c) For recombination through the empty states above E_{fo} and below E_{fn}, a different situation is obtained. Because n_R is increasing, p_R must be decreasing, and so $\beta>1$ will occur. We have not been able to obtain a simple expression for this case.

(d) If recombination is through the empty states above E_{fn}, we again have $\beta>1$. This occurs because

$$\Delta p_{t2} = \exp\left(-\Delta E_{fn/E_2}\right) \qquad (4.47)$$

and, therefore, $\Delta p_{t2}<1$. The value of β can be deduced from

$$\Delta G = \exp\left\{\frac{\Delta E_{fn}}{kT} - \frac{\Delta E_{fn}}{E_2}\right\} \qquad (4.48$$

and

$$E_2 = kT\beta/(\beta-1) \qquad (4.49)$$

These last two subcases have an interesting application to the PC temperature response as well. It has been reported that anomalous "bumps" occur in the PC temperature response (Vanier et al, 1981; Persans, 1982). These "bumps" can be interpreted as an increase in the lifetime of the electrons due to the sensitization of the sample caused by the presence of a second set of localized states below the midgap (Rose, 1963; Vanier et al, 1981). In this case the "bump" is due to the presence of a set of states with a smaller electron capture cross-section. In the example which we have presented, there is an increase in the lifetime because the n_R states increase in density, thus decreasing the density of empty capture centres. Of course, this model is dependent on the defect level which dominates the recombination traffic. Alternatively, this model may reveal a mechanism which initiates the transfer of holes from the class 2 states (above midgap) to the class 1 states (below midgap).

We may summarize this section by stating that many values of B are possible within this model, all of them occurring in a consistent manner. In the following section we shall analyze the observed PC intensity data. We analyze our data with our method and Evangelisti's method (Evangelisti et al, 1983) and determine how these methods are useful for different temperature and light intensity regimes.

4.2.2 Results and Discussion

Figure 4.6 shows the photoconductivity (PC) as a function of light intensity for sample 9.06. Most of the data has been approximated by using the straight lines. At lower intensities we observe $\beta \leq 0.50$, but at higher intensities a changeover occurs, and then $\beta \doteq 0.80$. We would expect that the change in the value of β would be dependent on temperature if the effect is due to the position of the Fermi level, however this behaviour is not observed. The cause of the changeover may be that the rate of recombination depends also on the electron density. In Figure 4.7 (a and b) are shown similar data, observed for sample 13H. At low intensities there is a region with $\beta < 0.5$, and at the temperatures near 300 K we have $\beta > 1$ for low intensities.

We have analyzed this data using two methods, and have obtained the density of states distribution for energies from E_{Fp} to 0.25eV below E_c, as shown in Figure 4.8. Clearly, there is a substantial difference between these two methods. Whereas Evangelisti's method (Evangelisti et al, 1983) obtains a minimum in the density of states (DOS) for both samples, we only observe that the distribution becomes uniform at energies closer to E_c. Our method is not sensitive to a minimum in the density of states, because we do not observe a consistent value of $B > 1$. However, our method could be sensitive to the minimum if we knew the absolute value of the density of states at some point in the gap. For instance, if we assume that $N_c = 10^{20}/cm^3$, and if we assume that $g(E_{fo}) = 10^{16}/cm^3$, then we can adjust

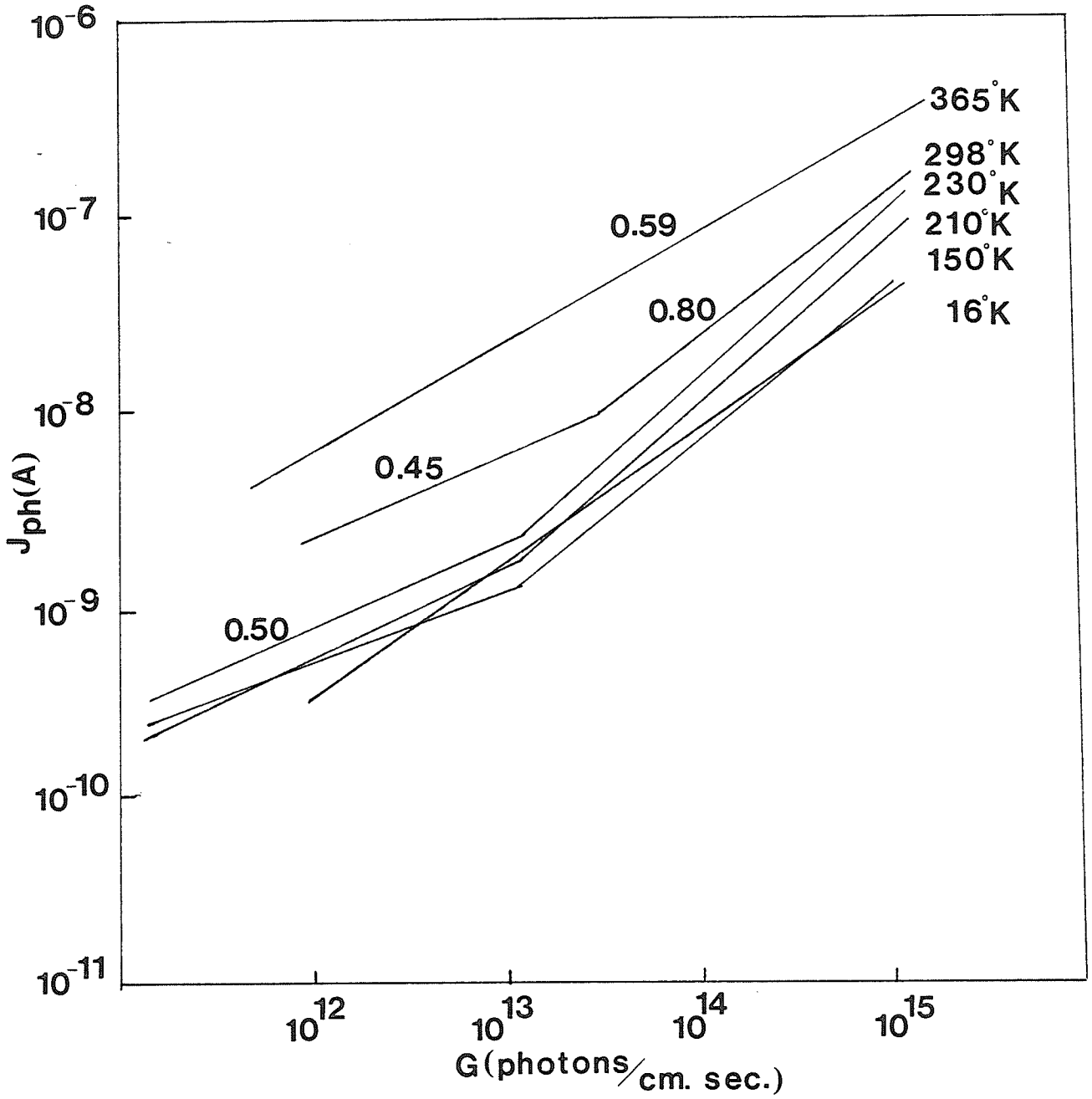

FIGURE 4.6. Response of the PC to light intensity.(Sample 9.06, hv= 1.96 eV)

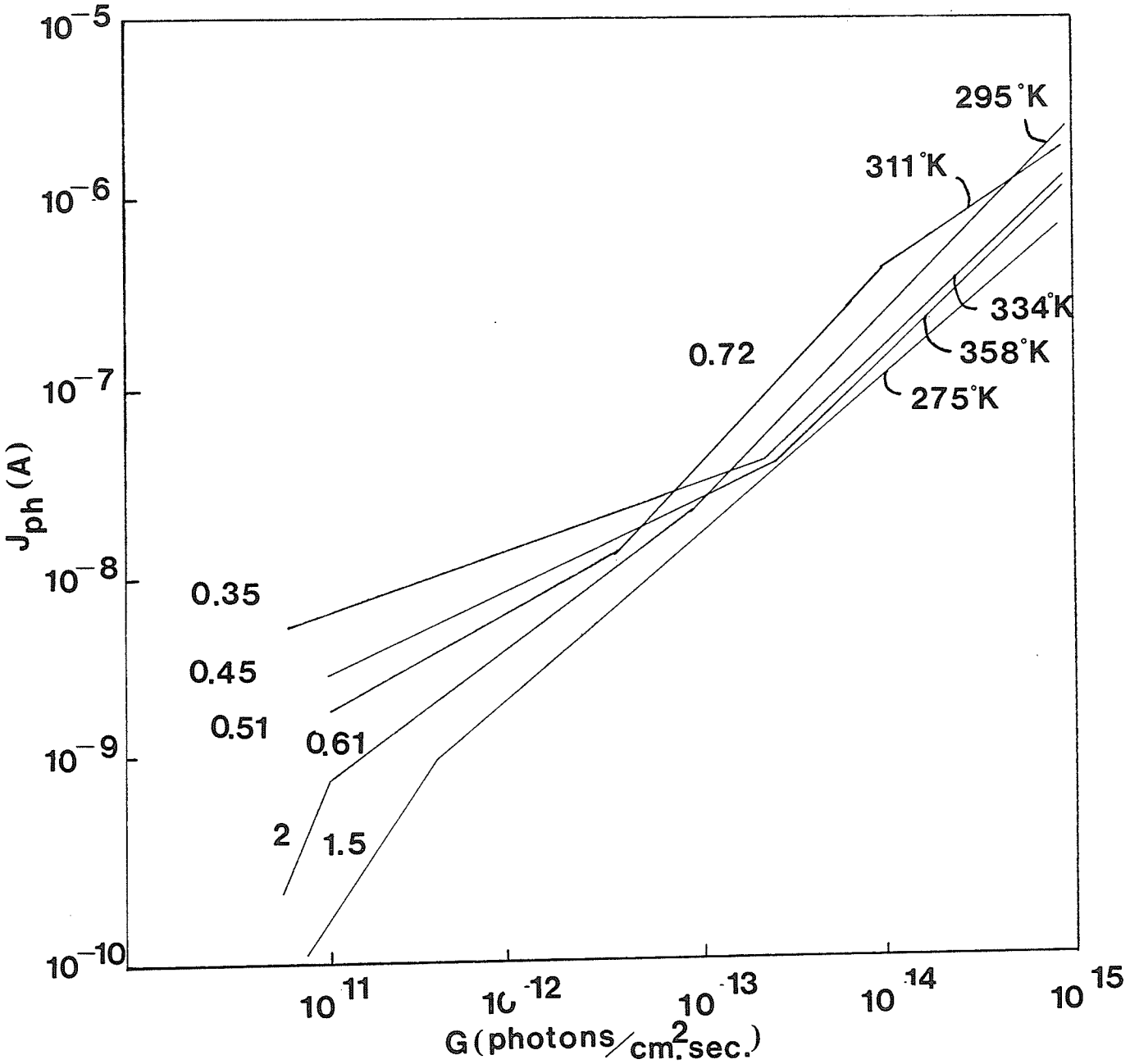

FIGURE 4.7.a) Response of the PC to light intensity.(Sample 13H, hv=1.96 eV). Data for high temperatures.

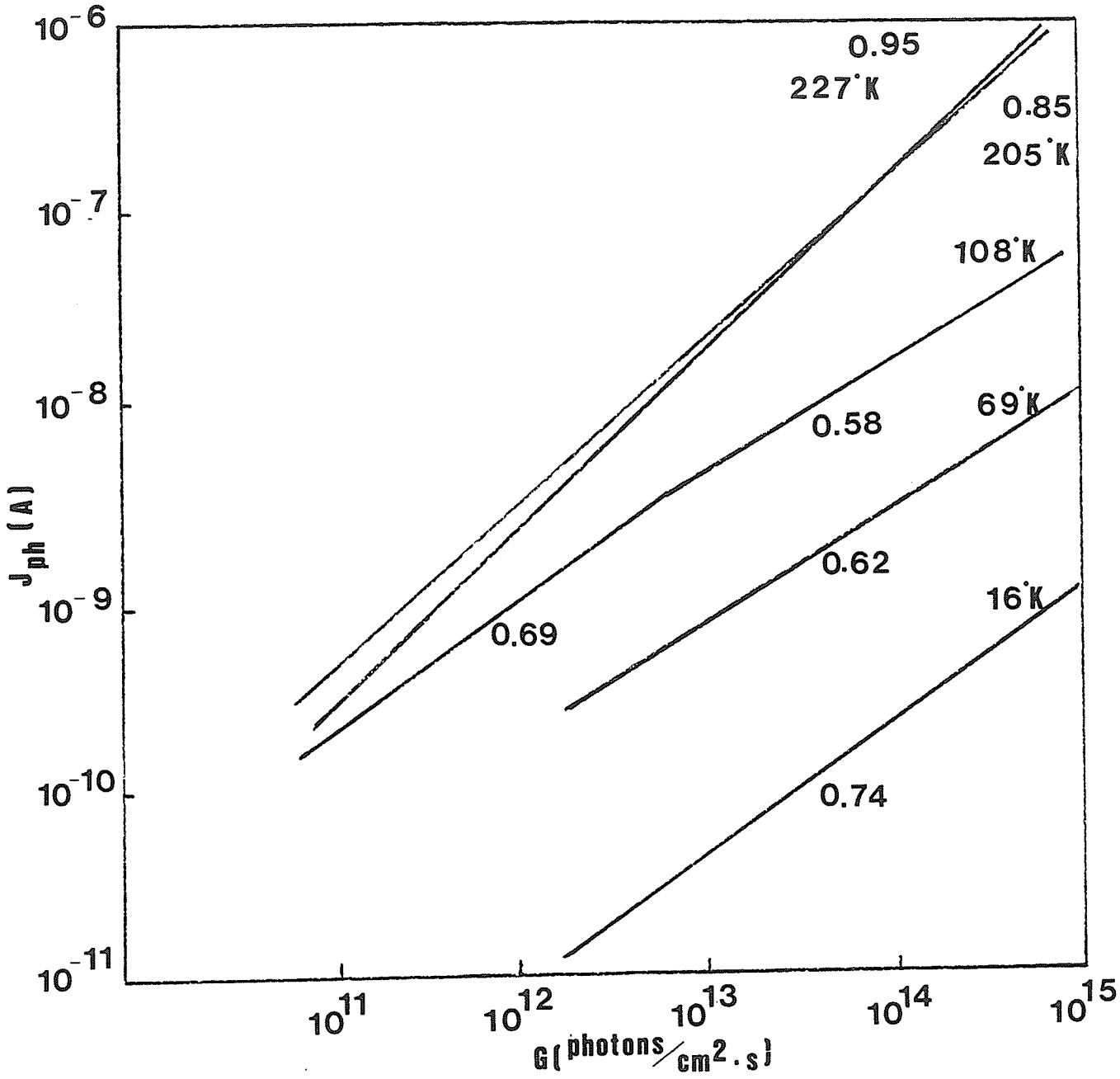

FIGURE 4.7. b) Response of the PC to light intensity. (sample 13H, hv = 1.96 eV). Data for low temperatures.

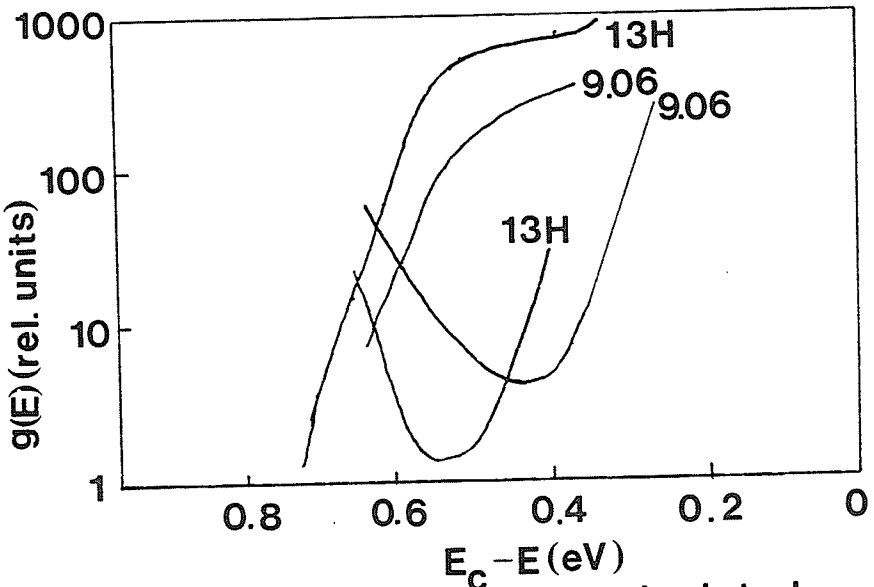

FIGURE 4.8. The calculated distribution of localized gap states.

our curves so that they fit these two values. We need more complete data to perform this adjustment with any accuracy.

In summary, we have proposed a new method of analysis for the light intensity dependence of the photoconductivity. The original result due to Rose (1963) has been reproduced. However, we have shown that it is also useful for analyzing the values $B<0.5$ and $B>1.0$. We have also shown that the distribution of states below the level E_{fo} also affect the behaviour of the photoconductivity. Further improvements to this theory would include the thermally generated carriers. Also, we mention that the approach we have presented is easily adapted for computer iteration, which will yield greater accuracy.

4.3 The Low Temperature Photoconductivity Maximum

In this section, we explain how the low temperature photoconductivity (PC) maximum can occur because of the structure of the localized gap state distribution. This analysis is new, in that it indicates how the "transfer" of holes from the states above E_{Fo} to the states below E_{Fo} is initiated. If the charge neutrality condition is dominated by trapped charge the maximum will not occur. In the following we review the relevant theory of this behaviour (Rose, 1963; Vanier et al, 1981), and show how our new approach "fits in" with this behaviour. We then present our experimental results, and determine some characteristics of the localized gap state distribution.

The temperature dependence of the photoconductivity (PC) often exhibits a maximum value in the temperature range of 280 K to 100 K (Vanier et al, 1981; Griffith et al, 1981; Persans, 1982). The temperature at which the maximum occurs shifts with light intensity, and usually a well-defined activation energy can be identified with this shift. To analyze this behaviour, the following model has been proposed (Rose, 1963), based on the density of states model shown in Figure 4.9. The class 1 states are below midgap, and have a small electron capture cross-section. The class 2 states above midgap have a larger electron capture cross-section, such that $\sigma_{2n} >> \sigma_{1n}$. The hole capture cross-sections are equal. We assume that $\sigma_{2n} = \sigma_{2p} = \sigma_{1p} = 10^{-15}\ cm^2$, and that $\sigma_{1n} = 10^{-19} cm^2$. Also, we assume tht $N_1 = N_2$, where N_1 and N_2 are the densities of the class 1 and class 2 states, respectively. At room temperature the class 2 states dominate the recombination, and thus the lifetime is expressed as

$$\tau_n = ((v\,\sigma_{n2})p_{R2})^{-1} \qquad (4.50)$$

where v is the microscopic velocity and p_{R2} is the density of empty recombination centres in the class 2 states. We assume that the class 2 population is determined by the recombination kinetics, and so the density of empty centres, based on the condition $R_n = R_p$ in steady-state, is (Rose, 1963)

$$p_{R2} = N_2 \left\{ \frac{1}{1 + \frac{\sigma_{n2} n}{\sigma_{p2} p}} \right\} \qquad (4.51)$$

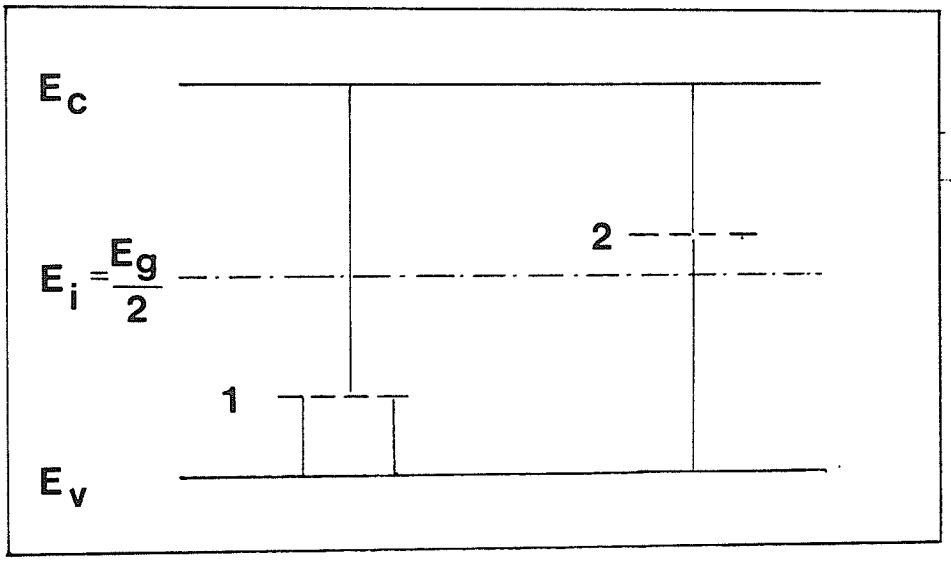

FIGURE 4.9 The discrete density of states model.

The density of empty centres is dependent on the density of defect states and the ratio of free electrons to free holes, because $\sigma_{n2} = \sigma_{p2}$.

If the temperature is now decreased, but the light intensity is maintained constant, then the PC will reach a minimum and then increases to a maximum value. This occurs as E_{fp}, the hole quasi Fermi level, decreases below E_1, thus changing the class 1 states from deep hole traps to recombination centres. These class 1 states have a small electron capture cross-section, which means that all the states are essentially empty. The value of the density of empty recombination centres for the class 1 states is

$$p_{R1} = N_1 \left\{ \frac{1}{1 + \frac{\sigma_{n1} n}{\sigma_{p1} p}} \right\} \tag{4.52}$$

Because the cross-sections are $\sigma_{n1} = 10^{-19}$ cm^2 and $\sigma_{p1} = 10^{-15}$cm^2, we have $p_{R1} \doteq N_1$. By charge neutrality we have (Rose, 1963)

$$n_{R2} = p_{R1} \tag{4.53}$$

where the filled class 2 states and the empty class 1 states are charged. We know by assumption that the total densities of the states are equal, and so $n_{R2} \doteq N_2 = N_1$. The lifetime may now be expressed as

$$\tau_n \doteq ((v \sigma_n) p_{R1})^{-1} \tag{4.54}$$

Therefore, the ratio of the maximum lifetime to the room temperature lifetime is

$$\Delta \tau_n = \frac{(10^7 \; 10^{-19} \; N_1)^{-1}}{(10^7 \; 10^{-15} \; \frac{N_2}{2})^{-1}} = 5 \times 10^5 \text{ seconds} \tag{4.55}$$

The lifetime has increased by almost six orders of magnitude. This analysis is based on the assumption that the charge neutrality equation can be written as

$$n_{R2} = p_{R1} \tag{4.56}$$

That is, we must neglect trapped charge.

As the light intensity changes, the position of both the minimum and the maximum shift to lower temperatures. The activation energy of this shift is important because it enables the determination of the energy level of the class 1 states. The activation energy of the PC maximum is equal to the sum of the activation energy of the mobility mechanism, W, and the activation energy of the recombination process. The recombination process involves the excitation of the electrons from the electron Fermi level to the conduction band edge, because we assume that only free electrons are able to recombine with trapped holes. However, the trapped holes can recombine without any excitation to the valence band, because we assume monomolecular recombination. Therefore, the activation energy of the maximum can be written as (Vanier et al, 1981)

$$E_1 - E_v = E_{max} - (E_c - E_2) + W \tag{4.57}$$

where $E_1 - E_v$ is the position of the class 1 states below midgap. This equation can also be used to analyze the data from materials with a continuous density of states. In this case the activation energy of the minimum yields the energy at which the class 1 distribution begins, and the activation energy of the maximum locates the end of the class 1 distribution.

For a-Si:H films, generally there are two sets of states at the Fermi level, and so if the class 1 states lie between $\sim$0.25eV to 0.50eV, then there are at least three types of states in the gap. We believe that the PC maximum can be explained with only two types of continuous states, and we present our analysis below.

In Figure 4.10 we show our model for a continuous distribution of gap states. There is a maximum and a minimum above the midgap. The total number of states above and below the midgap are the same, and the capture cross-sections have the same values as before, which means $\sigma_{1n} = 10^{-19}cm^2$, and $\sigma_{2n} = \sigma_{1p} = \sigma_{2p} = 10^{-15}cm^2$.

At high temperatures, for a given light intensity, the Fermi levels lie in the class 1 and class 2 states as shown. The recombination traffic proceeds through the class 2 states, because we choose $\sigma_{n2}\, p_{R2} >> \sigma_{n1} p_{R1}$. The charge neutrality is written as

$$p_{R1} = n_{t2} + n_{R2} \tag{4.58}$$

because we assume $p_{R1} >> p_{t1}$ for all temperatures. This assumption is valid because the density of empty states may be expressed.

$$P_{R1} = N_1 \left\{ \frac{1}{1 + \frac{\sigma_{n1} n}{\sigma_{p1} p}} \right\} \tag{4.59}$$

where we have $\sigma_{n1}/\sigma_{p1} = 10^{-4}$.

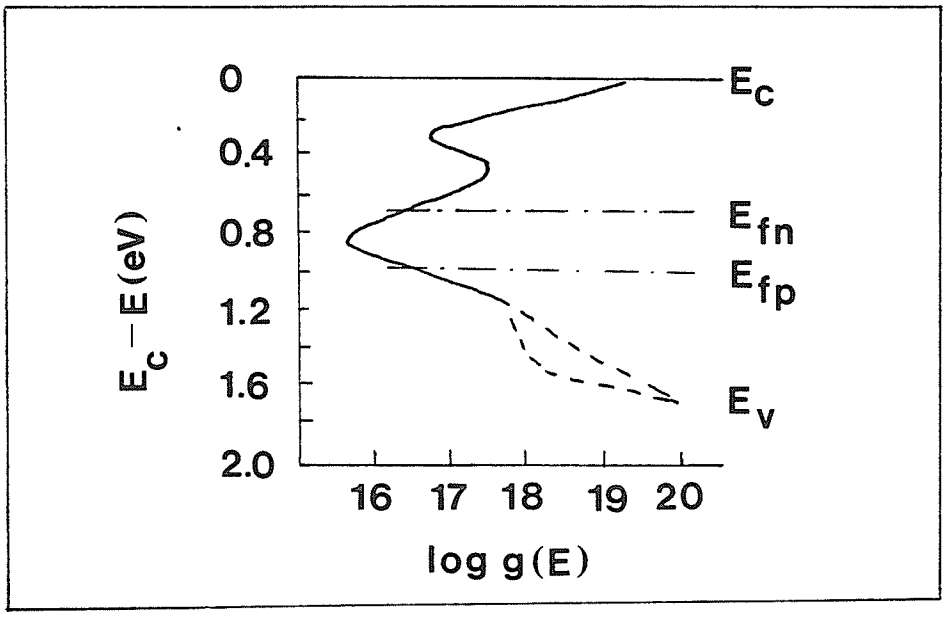

FIGURE 4.10 The continuous density of states model.

As the temperature decreases, the Fermi levels spread out from midgap, converting more of the class 1 and class 2 into recombination centres. The class 2 states above the midgap will not be completely filled with electrons, because $\sigma_{n2}/\sigma_{p2} = 1$, and so the lifetime will be decreasing. When the electron Fermi level reaches the density of states maximum, the density of trapped electrons begins decreasing from its previous value. However, the density of the positive charge continues increasing, and so the value of n_{R2} must increase to compensate for these changes. Therefore, the recombination rate decreases and the lifetime increases. It is this increasing lifetime that causes the PC minimum to occur.

For further decreases in temperature the electron Fermi level will eventually reach the density of states minimum, which is at an energy of 0.25eV below E_c. When this occurs, the trapped electron charge will again contribute an increasing amount to the charge neutrality condition, and therefore the density of filled centres, n_{R2}, can stop increasing. As the temperature continues decreasing the lifetime will again decrease, due to the added incorporation of class 2 states as recombination centres. This anslysis has assumed that the class 2 states dominate the recombination traffic for all temperatures.

Alternatively, it is possible that the states below the midgap, the class 1 states, begin to dominate the recombination when E_{Fn} reaches the maximum at 0.50eV below E_c. For E_{Fn} between 0.50eV and 0.25eV the

recombination traffic will move increasingly through the class 1 centres if their density is larger than the density of the class 2 states. When the minimum at 0.25eV below E_c is reached, the fraction of the recombination which proceeds through the class 1 states may reach a constant value.

In Figure 4.11 we present our results of the PC response to temperature. The activation energy of the minimum is 0.46eV and the activation energy of the maximum is 0.28eV. It can be seen that the slope of the low temperature side of the maximum decreases as the light intensity and temperature are reduced. The electron Fermi level is equal to 0.46eV at the PC minimum and $\sim$ 0.28eV at the PC maximum, for all light intensity levels. This value of E_{Fn} has been calculated using an activated mobility of

$$\mu_D = \mu_o \exp(-W/kT) \tag{4.60}$$

where W = 0.1eV for temperatures above $\sim$ 200°K but decreases gradually towards zero below 200°K.

According to the generally accepted theory, the energy range of the class 1 states is estimated to be (Vanier et al, 1981)

$$E_{1min} = 0.46 = 0.2 + 0.1 = 0.36eV \tag{4.61}$$

$$E_{1max} = 0.28 - 0.2 + 0.1 = 0.18eV \tag{4.62}$$

and therefore the distribution of class 1 states would begin at $\sim$0.18eV above E_v and extend up to 0.36eV above E_v. This is not a very broad distribution of states for an amorphous film.

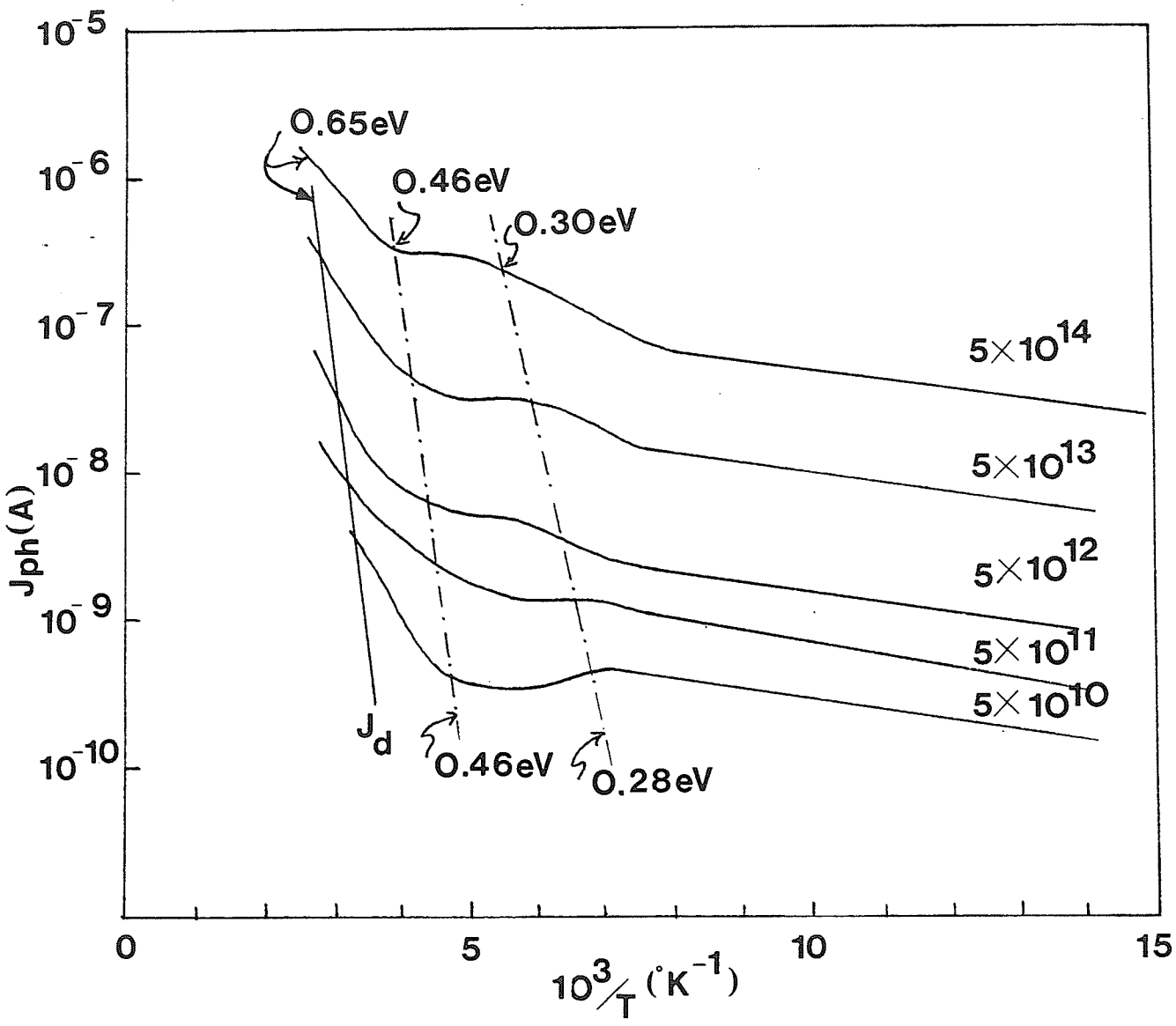

FIGURE 4.11. The PC response to temperature for several light intensities(Sample 9.06, hv=1.96 eV)

Based on our analysis, we can say that there is a maximum in the gap DOS at 0.46eV below E_c and a minimum in the gap DOS at 0.28eV below E_c, and that the density of class 1 states increases as the E_{fp} level moves towards the valence band edge.

In summary, the occurrence of the low temperature PC maximum can be attributed to the presence of a maximum and minimum in the density of states above midgap. Clearly, further improvements to this theory are possible, such as a mathematical expression to correlate the density of states to the form of the PC temperature response. These improvements are being attended to presently.

CHAPTER 5: CONCLUSIONS

From the analysis that has been presented in chapters three and four we can make the following conclusions. Firstly, the orientation and position of the samples during deposition are very important for the structure of the film. This is revealed in section 4.1, where the samples 9.06 and 9.08 display drastically different properties, although they are prepared under the same conditions. The only difference is their position in the chamber. Also, samples 13H and 13V are different only in their orientation, one being vertical and the other horizontal.

Secondly, it is clear that the size of the microcrystallites depends on the value of the magnetic field. As well, it is possible that the 20Å microcrystallite size is preferentially grown near the ECR condition. The influence of the deposition parameters on the film characteristics will, of course, be a subject of continuing study.

Thirdly, sections 4.2 and 4.3 enable us to find the position of the maximum and minimum above the equilibrium Fermi level. For sample 9.06 the maxima is located at 0.46eV below E_c and the minimum is located 0.28eV below E_c. This structure in the states above the midgap has been shown to lead to a low temperature PC maximum.

Fourthly, we have shown that a new interpretation of the PC intensity dependence is possible. This analysis method involves using the

charge neutrality and two sets of continuous states in the gap. One distribution of states is above the Fermi level and the other is below the Fermi level. We have shown that all of the values of β can be analyzed using these equations.

Overall, therefore, it is possible to measure the distribution of the gap states using the PC intensity response and the PC temperature response, in the temperature range of 350°K to 100°K.

APPENDIX

Here we review the preparation conditions used for these films, and present the necessary information about the experimental apparatus and methods. The review of these methods is informal, and hopefully future experimental mistakes can be avoided by these notes.

A1. Deposition Conditions

The fabrication system consists of a waveguide suitable for microwave propagation, an oscillator at a frequency of 2.45 GHz, a gas delivery system, and two axially oriented solenoids which develops a magnetic field of up to 1 KGauss. This magnetic field is used to confine the plasma and control the energy of the electrons. The fabrication facility has been reviewed in previous reports (Mejia et al, 1982; 1986).

The deposition conditions were essentailly constant for all the films from run 10 to run 13, with the exception of the magnetic field. The magnetic field is allowed to vary from low values, which are below electron cyclotron resonance (ECR), to high values above ECR. We also observe that the microwave power absorbed by the plasma changes for these runs. This variation could not be avoided, but we expect that the affect of this change is small. For run 9, the temperature of the substrate has been increased to 200 C. This is shown by the crystallite size values.

A2. Experimental Procedure

PC Spectral Response - We used a tungsten filament, and selected wavelengths with a monochromater. We did not achieve good collimating of the light beam in our setup, so this can be an improvement in future work. A variac may be connected to the light source, so that a constant intensity or photon flux may be maintained. For wavelengths above 750 nm, a long-pass filter must be used, so that the second order modes from the diffraction gratings do not cause errors.

There is some speculation that illumination of the contacts will also affect the photocurrent, and thus cause errors unless accounted for. We did not find this to be a problem. To effectively exclude contact effects we could either mask the contacts with paint or adjust the light spot size with a lens. We have not found paint to be useful, and the lens is easy to use only for well controlled (ie. collimated) beams. We managed to measure the PC with and without illuminated contacts, and found that there are no differences.

PC Temperature Dependence - We use the cryogenic unit, which controls the temperature from 16 K to 380 K. The choice of electric field is important, as we don't want to decrease the temperature and enter into a space-charge regime. Also, we measured the PC for both increasing and decreasing temperature, and therefore eliminated the possibility of thermally stimulated affects.

PC Intensity Dependence - The intensity dependence of the PC is easily measured by using neutral density filters. The dark conductivity must be subtracted from the photoconductivity, and for the lower intensities and lower temperatures there is an increase in the time required to reach steady-state. Therefore, more time is allowed for the PC to reach steady state.

BIBLIOGRAPHY

B. Abeles, C.R. Wronski, T. Tredje and G.D. Cody, Sol. St. Comm., 36, 537-540 (1980)

D. Adler, M. Silver, A. Madan and W. Czubatyj, J. Supp. Phys., 51, 12, 6429-6431 (1980)

D.A. Anderson and W.E. Spear, Phil. Mag., 36, 3, 695-712 (1977)

V.I. Arkhipov, J.A. Popova and A.I. Rudenko, Phil. Mag. B, 58, 5, 401-410 (1983)

T.C. Arnoldussen, R.H. Bube, E.A. Fagen and S. Holmberg, J. Appl. Phys., 43, 4, 1798-1807, (1972)

P.K. Bhat, D.J. Dunstan, I.G. Austin and T.M. Searle, J. Non-Cryst. Sol., 59-60, 349-352 (1983)

J.S. Blakemore, Can. J. Phys., 34, 938-1148 (1956)

J.S. Blakemore and C.E. Sarver, Phys. Rev., 173, 3, 767-774 (1968)

R.H. Bube, "Photoconductivity of Solids", (Wiley, New York, 1960)

F. Carasco and W.E. Spear, Phil. Mag. B, 47, 5, 495-507 (1983)

R.C. Chittick, J.H. Alexander and H.F. Sterling, J. Electrochem. Soc., 116, 77, (1969)

G.D. Cody, B. Abeles, C.R. Wronski, B. Brooks and W.A. Lanford, J. Non-Cryst. Sol., 35-36, 463-468 (1980)

R.S. Crandall, J. Non-Cryst. Sol., 35-36, 381-386, (1980); in "Semiconductors and Semimetals", 21, D (Academic Press, Orlando, 1984)

B.D. Cullity, "Elements of X-ray Diffraction", (Addison-Wesley, Reading, 1956), ch. 17.

T. Datta and M. Silver, Sol. St. Comm., 38, 1067-1971 (1981)

H. Dersch, L. Schweitzer and J. Stuke, Phys. Rev. B, 28, 8 4678-4684 (1983)

F. Evangelisti, P. Fiorini, G. Fortunato and C. Giorannella, Sol. St. Comm., 47, 2, 107-110 (1983a)

F. Evangelisti, P. Fiorini, G. Fortunato, A. Frova, C. Giovannella and R. Peruzzi, J. Non-Cryst. Sol., 55, 191-201 (1983b)

Furukawa, T. Kagawa and N. Matsumoto, Sol. St. Comm., 44, 927 (1982)

J. Geiger, Phil. Mag. B., 51, 3, L33-L38 (1985)

A.M. Goodman and A. Rose, J. Appl. Phys., 42, 7, 2823-2830 (1971)

N. Goodman and H. Fritzsche, Phil. Mag. B., 42, 149 (1980)

R.W. Griffith, F.J. Kampas, P.E. Vanier and M.D. Hirsch, J. Non-Cryst. Sol., 35-36, 391-396 (1980)

M. Hack, S. Guha, and M. Shur, Phys. Rev. B., 30, 12, 6991-6999 (1984)

Y. Hamakawa, Japan. Ann. Rev. (Amorph. Semicond.), 16, 2, (1984)

T. Hamasaki, H. Kurata, M. Hirose and Y. Osaka, Appl. Phys. Lett., 37, 1084 (1980)

M. Hirose, Japan. Ann. Rev. (Amorph. Semicond.) 34, (1982)

H.J. Hoffman and F. Stockmann, in Festkorperprobleme (Advances in Solid State Physics), XIX, (Vieweg, Wiesbaden, 1979), p.271

M. Hoheisel, R. Carius, and W. Fuhs, J. Non-Cryst. Sol., 63, 313-319 (1984)

Z. Iqbal and S. Veprek, J. Phys. C: Sol. St. Phys., 15, 377 (1982)

T. Kagawa and N. Matsumoto, J. Non-Cryst. Sol., 59-60, 465-478 (1983)

H.P. Klug and L.E. Alexander, "X-ray Diffraction Procedures", Wiley, New York, 1954), ch.6.

K.V. Kougiya, A.I. Kosarev, A.A. Andreev, M.M. Mezdrogi na, A.A. Rodina, and D.P. Utkin-Edin, Sov. Phys-Semicond., 14, 12, 1424-1425 (1980)

R.E. Lagos, H. Suhl, and T. Tiedje, I. Appl. Phys., 54, 7, 3951-3957 (1983)

P.G. LeComber and J. Mort, "Electronic and Structural Properties of Amorphous Semiconductors", (Academic Press, London, 1973)

P.G. LeComber, G. Willeke and W.E. Spear, J. Non-Cryst. Sol., 59-60, 795 (1983)

R.J. Loveland, W.E. Spear, and A. Al-Sharbaty, J. Non-Cryst. Sol., 13, 55-68 (1974)

A. Matsuda, J. Non-Cryst. Sol., 59-60, 767 (1983)

S.R. Mejia, R.D. Mcleod, K.C. Kao and H.C. Card, J. Non-Cryst. Sol., 13, 55-68 (1984)

S.R. Mejia, R.D. Mcleod, W. Pries, P.K. Shufflebotham, D.J. Thomson, J.F. White, J.J. Schellenberg, K.C. Kao, and H.C. Card, J. Non-Cryst. Sol., 77-78 765-768 (1985)

A.G. Milnes, "Deep Impurities in Semiconductors", (Wiley, New York, 1973)

Y. Mishima, S. Miyazaki, M. Hirose and Y. Osaka, Phil. Mag. B., 46, 1, (1982)

D.S. Misra, A. Kumar and S.C. Agarwal, Phys. stat. sol. (a), S5, 297 (1984)

G. Moddel, D.A. Anderson and W. Paul, Phys. Rev. B, 22, 4, 1911-1925 (1980)

N.F. Mott and E.A. Davis, "Electronic Processes in Non-crystalline Materials", (Clarendon, Oxford, 1979)

T.D. Moustakas, Sol. St. Comm., 35, 745-751 (1980)

M. Noda, H. Shimuzi, H. Kohno and H. Ishida, J. Non-Cryst. Sol., 59-60, 823 (1983)

S. Oda, Y. Soito, I. Shimuzi and E. Inoue, Phil. Mag. B., 43, 6, 1079-1089 (1981)

Y. Osaka and T. Imura, Japan. Ann. Rev., 16, 80, (1984)

H. Overhof and W. Beyer, Phil. Mag. B., 43, 3, 433-450 (1981)

J.I. Pankove, F.H. Pollak and C. Schnabolk, J. Non-Cryst. Sol., 35-36, 459-462 (1980)

P.D. Persans, Sol. St. Comm., 36, 851-856 (1980); Phil Mag. B., 46, 5, 435-471 (1982)

W. Pickin, Solar Cells, 9, 85-111 (1983)

A. Rose, "Concepts in Photoconductivity and Allied Problems", (Wiley, New York, 1963)

J. Shirafuji, M. Kawagaki and S. Nagata, J. Non-Cryst. Sol., 72, 199-210 (1984)

J.G. Simmons and G.W. Taylor, J. Non-Cryst. Sol., 8-10, 947-953 (1972); J. Phys. C: Sol. St. Phys., 7, 3051-3066 (1974)

W.E. Spear, G. Willeke, P.G. LeComber and A.G. Fitzgerald, J. de Physique, supp. 10, C4, 257 (1981)

R.A. Street, Phil. Mag. B., 49, 1, L15-L20 (1984)

K. Tanaka and A. Matsuda, Japan. Ann. Rev., 6, 161 (1983)

G.W. Taylor and J.G. Simmons, J. Non-Cryst., Sol., 8-10, 940-946 (1972); J. Phys., C: Sol. St. Phys., 7, 3067-3074 (1974)

T. Tiedje and J.M. Celbulka, Phys. Rev. B., 28, 12, (1983)

M. Vanacek, J. Kocka, J. Stuchlik and A. Triska, Sol. St. Comm., 39, 1199-1202 (1981)

P.E. Vanier, A.E. Delahot and R.W. Griffith, J. Appl. Phys., 52, 8, 5235-5242 (1981)

P.E. Vanier and R.W. Griffith, J. Appl. Phys., 53, 4, 3098-3102 (1982)

Z. Vardeny and J. Tauc, Phys. Rev. Lett., 46, 18, 1223-1226 (1981)

S. Veprek and V. Maracek, Sol. St. Electron., 11, 683 (1968)

C.R. Wronski and R.E. Daniel, Phys. Rev. B, 23, 2, 794-804 (1981)

P.J. Zanzucchi, C.R. Wronski and D.E. Carlson, J. Appl. Phys., 48, 12, 5227-5236 (1977).